Beyond the CpG: an integrative approach to decoding DNA methylation in immunometabolic health

Sinke, L.J.

CHAPTER THREE

Adipokines

DNA methylation of genes involved in lipid metabolism drives adiponectin levels and metabolic disease

Lucy Sinke[1], Thomas Delerue[2], Rory Wilson[2], Xueling Lu[3,4], Yujing Xia[5], Ricardo Costeira[5], M. Kamal Nasr[6,7], Marian Beekman[1], Lude Franke[3], Alexandra Zhernakova[3], Jingyuan Fu[3], Christian Gieger[2,8], Christian Herder[9,10], Wolfgang Koenig[8,11,12], Annette Peters[2,8,13], Jose M. Ordovas[14], Marcus Dörr[6,7], Hans J. Grabe[6], Matthias Nauck[6,7], Jordana T. Bell[5], Alexander Teumer[6,7,15], Harold Snieder[3], Melanie Waldenberger[2,8], P. Eline Slagboom[1], and Bastiaan T. Heijmans[1]

[1] Leiden University Medical Centre, Leiden, The Netherlands
[2] Helmholtz Munich, Neuherberg, Germany
[3] University of Groningen, Groningen, The Netherlands
[4] Shantou University Medical College, Guangdong, China
[5] King's College London, London, United Kingdom
[6] University Medicine Greifswald, Greifswald, Germany
[7] German Centre for Cardiovascular Research (DZHK), Greifswald, Germany
[8] German Centre for Cardiovascular Research (DZHK), Munich, Germany
[9] Heinrich Heine University Düsseldorf, Düsseldorf, Germany
[10] German Centre for Diabetes Research (DZD), Neuherberg, Germany
[11] Technical University of Munich, Munich, Germany
[12] Ulm University, Ulm, Germany
[13] Ludwig Maximilian University of Munich, Munich, Germany
[14] Tufts University, Boston, Massachusetts, United States of America
[15] German Centre for Neurodegenerative Diseases (DZNE), Greifswald, Germany

Published in Diabetologia 69, 127-145 (2026)
DOI: 10.1007/s00125-025-06549-6

Abstract

Despite playing critical roles in the pathophysiology of metabolic disorders such as type 2 diabetes (T2D), the molecular mechanisms underlying circulating adipokine levels remain poorly understood. By identifying genomic regions involved in the regulation of adipokine levels, we can improve our understanding of T2D pathogenesis and inter-individual differences in metabolic disease risk.

We conducted an epigenome-wide meta-analysis of associations between serum adiponectin (*n* = 2,791) and leptin (*n* = 3,661), and leukocyte DNA methylation at over 400,000 CpG sites across five European cohorts. The resulting methylation signatures were followed up using functional genomics, integrative analyses, and causal inference. Our findings revealed robust associations with adiponectin at 73 CpGs and with leptin at 211 CpGs. Many identified sites were associated with metabolic syndrome risk factors, located in regulatory chromatin regions, and correlated with genes important for lipid transport (e.g. *ABCG1*), metabolism (e.g. *CPT1A*), and biosynthesis (e.g. *DHCR24*).

Bidirectional two-sample Mendelian randomisation further identified two specific sites as plausible drivers of both adiponectin levels and metabolic health: one annotated to *ADIPOQ*, the gene encoding adiponectin, and another linked to *SREBF1* expression, an established modifier of T2D risk known to exert its effects via adiponectin. Taken together, this large-scale and integrative analysis uncovers links between adipokines and widespread yet functionally specific differences in gene regulation with a central role in T2D and its risk factors.

Graphical Abstract

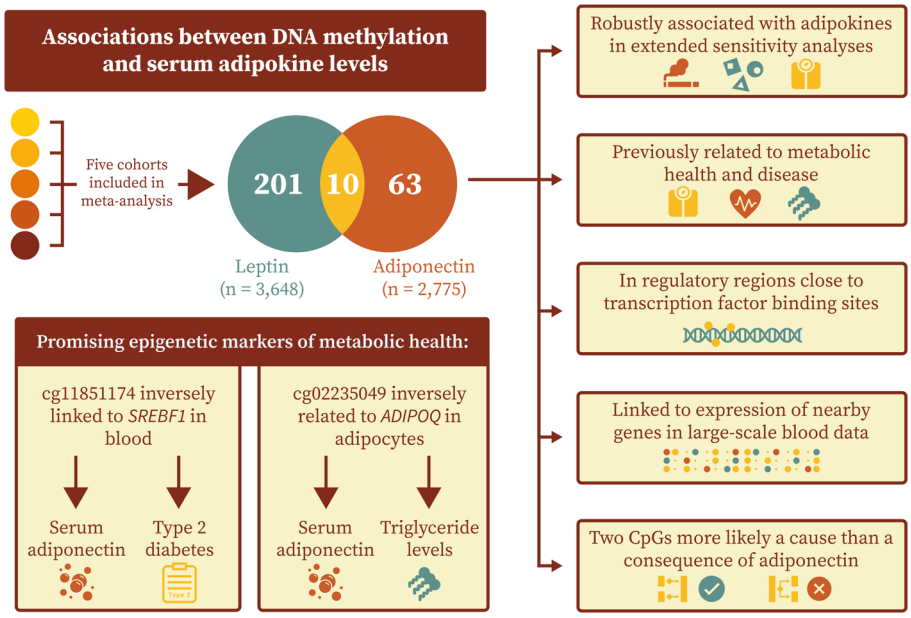

Highlights

- 73 CpGs associate with adiponectin and 211 CpGs link to leptin in blood.
- These CpGs are enriched for residing in enhancers close to relevant transcription factor binding sites.
- Integrative analyses connect adipokine-associated DNA methylation to genes involved in lipid transport, metabolism, and synthesis.
- Triangulation supports DNA methylation at identified CpGs as plausibly driving adiponectin production.
- In line with this, two-sample Mendelian randomisation identifies two putatively causal sites: one at *ADIPOQ*, and another at *SREBF1*.
- Public data uncovers correlation between *ADIPOQ* expression and DNAm at the implicated CpG in adipocytes, the primary producers of adiponectin.
- We propose that shared upstream factors, such as diet, could be inducing tissue-agnostic DNAm effects, enabling large-scale blood-based EWAS to pinpoint regulatory sites even for traits non-hematopoietic in origin.

Keywords: *adiponectin, causal inference, epigenomics, leptin, lipid metabolism, meta-analysis, metabolic health, type 2 diabetes*

Background

Adiponectin and leptin are two adipokines that play central roles in regulating energy homeostasis and metabolism, with influences on both insulin sensitivity and inflammation. Circulating levels of these molecular mediators are directly implicated in the pathogenesis and progression of the metabolic syndrome and type 2 diabetes (T2D). A clearer understanding of their regulation could therefore uncover new avenues for predicting, preventing or treating metabolic disease[1,2].

Epigenetic modifications, such as DNA methylation (DNAm), are established as being both responsive to lifestyle changes and capable of modifying disease risk. Growing evidence also supports epigenetic regulation of adiponectin and leptin specifically as partly driving inter-individual differences in health[3,4]. Blood-based epigenome-wide association studies (EWAS) have previously uncovered robust and biologically coherent correlations between DNAm and metabolic risk factors, even where the investigated traits were non-haematopoietic in origin[5,6]. Supported explanations for detecting such associations in leukocytes include shared upstream drivers such as diet[7], DNAm responses to circulating phenotypes[8], and immune cell mediation of the inflammatory components of metabolic disease[9].

Despite substantial progress, however, research directly examining relationships between adiponectin and DNAm have been limited in sample size[10], and leptin has thus far not been investigated on a genome-wide scale. A comprehensive EWAS of these adipokines in a sufficiently large sample size is warranted to detect subtle but consistent molecular effects. Thorough interpretation of the resulting methylation signatures represents a critical next step in understanding the regulatory architecture of metabolic homeostasis in human health.

Results

Circulating adipokines have largely distinct DNA methylation signatures in blood

We performed EWAS meta-analyses of circulating adiponectin (n = 2,791; 412,224 CpGs) and leptin (n = 3,661; 406,390 CpGs) levels in blood samples from five European cohorts (**Table 1,2**). Mean age was 55.5 years in the leptin analysis and 56.8 years for adiponectin, and the population was predominantly female (adiponectin: 55.2%; leptin: 54.4%). Cohorts represented a combination of fasted (KORA, TwinsUK, SHIP-TREND, and LLD) and non-fasted (LLS) samples. The top 20 CpGs for each adipokine are provided in **Supplementary Tables 1** and **2**.

Characteristic	KORA F4	LLS	LLD	TwinsUK	SHIP-TREND
Sample size	807	718	701	124	441
Age, years	68.8 ± 4.4	58.9 ± 6.7	45.5 ± 13.1	55.1 ± 11.7	50.0 ± 13.4
Sex, female	396 (49.1)	370 (51.5)	411 (58.6)	124 (100.0)	241 (54.6)
BMI, kg/m^2	26.4 (4.2)	25.1 (4.3)	24.7 (4.8)	25.0 (4.7)	27.2 (4.2)
Smoking, current	69 (8.6)	85 (11.8)	130 (18.5)	28 (22.6)	154 (34.9)
Smoking, never	388 (48.1)	199 (27.7)	332 (47.4)	65 (52.4)	173 (39.2)
Adiponectin, µg/ml	9.7 (8.0)	5.3 (3.8)	3.7 (2.7)	7.2 (5.0)	7.0 (5.0)

Table 1 | Characteristics of the five cohorts included in the adiponectin EWAS meta-analysis. Values are shown as mean ± standard deviation for age (in years), as median (IQR) for adiponectin levels (in µg/mL) and body mass index (BMI; in kg/m^2), and as total (%) for sex and smoking status.

Characteristic	KORA F4	LLS	LLD	TwinsUK	SHIP-TREND
Sample size	1702	723	701	94	441
Age, years	60.9 ± 8.9	58.9 ± 6.7	45.5 ± 13.1	55.1 ± 11.9	50.0 ± 13.4
Sex, female	874 (51.4)	372 (51.4)	411 (58.6)	94 (100.0)	241 (54.6)
BMI, kg/m^2	27.4 (4.6)	25.1 (4.3)	24.7 (4.8)	25.0 (4.3)	27.2 (4.2)
Smoking, current	247 (14.5)	85 (11.8)	130 (18.5)	12 (12.8)	154 (34.9)
Smoking, never	711 (41.8)	199 (27.5)	332 (47.4)	50 (53.2)	173 (39.2)
Leptin, ng/ml	13.3 (19.9)	12.1 (20.6)	10.0 (17.0)	15.1 (12.1)	10.1 (14.7)

Table 2 | Characteristics of the five cohorts included in the leptin EWAS meta-analysis. Values are shown as mean ± standard deviation for age (in years), as median (IQR) for leptin levels (in ng/mL) and body mass index (BMI; in kg/m^2), and as total (%) for sex and smoking status.

Circulating levels of adiponectin and leptin were associated with blood-based DNAm at 73 CpG sites and 621 CpG sites, respectively ($p_{FDR} \leq 0.05$, nominal *p*-value thresholds 8.8e−6 for adiponectin, 7.6e−5 for leptin). These results were adjusted for age, sex, technical covariates, and six immune cell types predicted from DNAm data (granulocytes, monocytes, NK cells, CD4+ T cells, CD8+ T, cells and B cells). No CpGs displayed high heterogeneity between cohorts ($I^2 < 80\%$) and test statistics were corrected for bias and inflation.

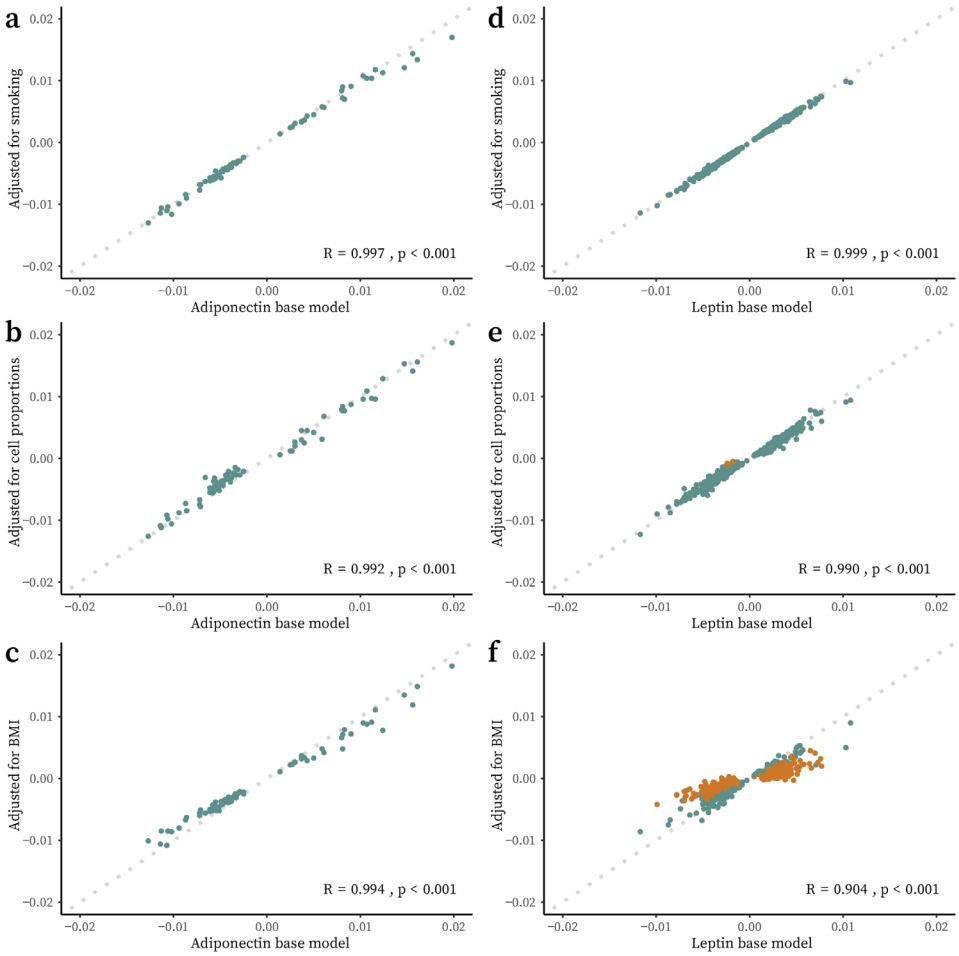

Figure 1 | Relationships between adipokine-associated DNAm effects before and after sensitivity analyses with Pearson correlation coefficients and associated *p*-values. Each point represents a CpG coloured by if they were taken forward in downstream analyses (blue) or removed (orange). A dotted reference line (y = x) indicates no change between models. **a)** Adiponectin-associated effects before and after adjustment for smoking, **b)** for twelve predicted blood-cell-type proportions, **c)** and for body mass index (BMI). **d)** Leptin-associated effects before and after adjustment for smoking, **e)** for twelve predicted blood-cell-type proportions, **f)** and for BMI.

To evaluate the stability of associations between DNAm and adipokines, base models were further adjusted for smoking status, twelve distinct cell types, and body mass index (BMI). For all of the adiponectin CpGs, associations remained statistically significant in these sensitivity analyses ($p_{FDR} \leq 0.05$), with strong correlations between effect sizes before and after adjustment ($R > 0.99$, $p < 0.001$; **Fig. 1a-c**).

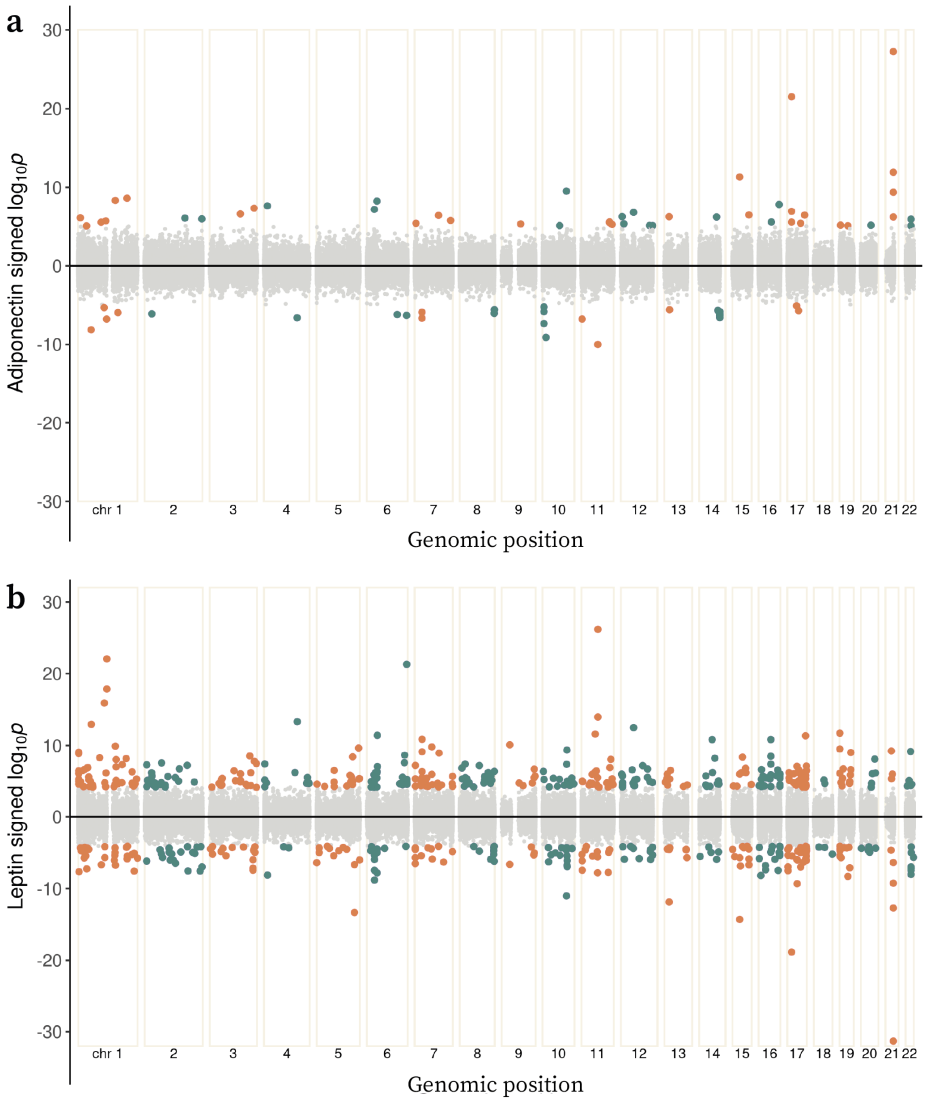

Figure 2 | Bidirectional Manhattan plots of the signed log_{10}p-values for all tested CpGs against their genomic position. CpGs significant at the 5% level after adjusting for multiple testing are shown in orange (odd-numbered chromosomes) or blue (even). Non-significant CpGs are shown in grey. **a)** Results from the adiponectin EWAS meta-analysis, and **b)** from the leptin EWAS meta- analysis.

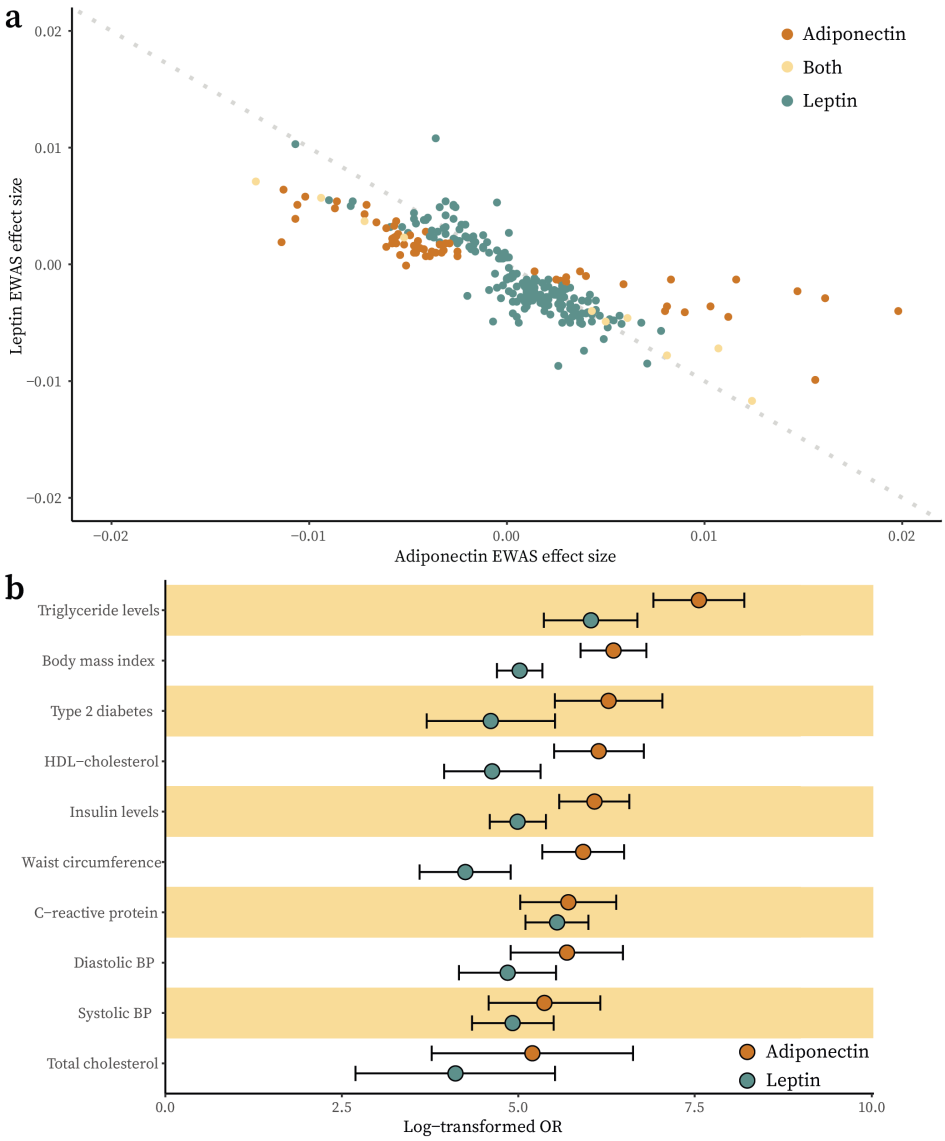

Figure 3 | Relationships between EWAS of different traits. a) Scatter plot of EWAS meta-analysis effect sizes for adiponectin and leptin for all CpGs significant at the 5% level in one or both analyses. A dotted reference line (y = −x) indicates perfectly inverse correlation between the two adipokines. **b)** Forest plot of trait enrichment in the adipokine-associated CpGs showing natural log-transformed ORs and their 95% CIs. Traits that are in the top ten (as determined by OR) for one or both adipokines are included, ordered by maximum OR. All enrichments shown are significant at the 5% level after adjusting for multiple testing.

Effects at leptin CpGs also showed relative independence from smoking and cell-type proportions (**Fig. 1d,e**). Unsurprisingly however, since leptin has stronger and more direct links to obesity[11,12], 401 leptin CpGs were sensitive to BMI adjustment ($p_{FDR} \geq 0.05$; **Fig. 1f**). To ensure focus on adipokine-specific epigenetic links in downstream analyses, these were removed from the results.

The final set of CpGs included 73 adiponectin (**Fig. 2a**) and 211 leptin-associated sites (**Fig. 2b**), representing 65 and 203 distinct loci, respectively. Ten CpGs were associated with both adipokines, and adiponectin and leptin effect sizes were inversely correlated at the 274 uniquely identified CpGs ($R = -0.81$ $p < 0.001$; **Fig. 3a**).

Adipokine-associated methylation is robustly connected to metabolic health

To assess the relevance of the adipokine-associated CpGs to human health and disease, we conducted a search of previous EWAS results (**Supplementary Table 3,4**). Notably, 65 of the 73 adiponectin CpGs (89.0%) and 145 of the 211 leptin CpGs (68.7%) were also associated with at least one other trait. As anticipated *a priori*, adipokines and adiposity were closely related (BMI ORs 571.7 and 151.3 for adiponectin and leptin, respectively; $p_{FDR} < 0.001$). In total, 40 (54.8%) of the adiponectin and 51 (24.2%) of the leptin CpGs were associated with BMI in large-scale blood-based EWAS. This was despite the removal of CpGs no longer significant after adjusting for BMI, supporting shared but independent epigenetic signals underlying BMI and the relevant adipokine at the remaining CpGs. Enrichments also existed for other metabolic risk factors, including HDL-cholesterol (ORs 465.8 and 102.8, $p_{FDR} < 0.001$), triglycerides (ORs 1917.4 and 413.7, $p_{FDR} < 0.001$), systolic BP (ORs 215.2 and 137.4, $p_{FDR} < 0.001$), fasting insulin (ORs 435.5 and 147.5, $p_{FDR} < 0.001$) and glucose levels (ORs 121.4 and 22.0, $p_{FDR} < 0.001$), as well as T2D itself (ORs 533.8 and 100.6, $p_{FDR} < 0.001$), highlighting the relevance of our CpGs to metabolic health as a whole (**Fig. 3b**).

Functional genomics uncovers regulatory potential for adipokine-associated CpGs

We annotated the genomic positions of the 73 adiponectin- and 211 leptin-associated CpGs to 15 chromatin states using Roadmap reference epigenomes[13]. These consist of eight active and seven repressed configurations showing distinct levels of DNAm, accessibility and regulator binding. By testing if adipokine CpGs were enriched for any particular genomic feature in the PBMC reference (E062), we revealed that active chromatin annotations were over-represented and repressive states depleted in our results (**Fig. 4a, Supplementary Table 5,6**).

Both adipokines displayed enhancer enrichment, with 18 adiponectin (24.7%, OR = 8.82) and 33 leptin CpGs (15.6%, OR = 4.87) annotated to enhancers, compared with only 3.6% of total tested CpGs in the adiponectin (n = 14,706) and leptin (n = 14,548)

analyses. This indicated high probability of colocalisation with markers of open chromatin, specifically H2K4me1[14]. To investigate whether this pattern was cell-type specific, enrichment was analysed using reference epigenomes for 22 other immune cell types (Roadmap Epigenomes: E029–48, E050–51) and adipocytes (E063). In all tested epigenomes except one (Treg for adiponectin), CpG genomic locations were enriched for enhancers ($p_{FDR} \leq 0.05$) demonstrating robust regulatory potential across immune and adipose cellular identities.

As the primary mechanism by which DNAm influences nearby expression is by modulating TF binding[15], we tested regions within 50 bp of the adipokine-associated CpGs for TFBS enrichments, revealing links to 14 distinct TFs (**Fig. 4b, Supplementary Table 7**). Several of these were central to immunity and inflammation (e.g. BATF and AP-1)[16-18], while others had specific adipokine relevance, including Fosl2, which promotes leptin expression[19], and MafA, which downregulates adiponectin[20]. Taken together, these functional analyses supported adipokine-related DNAm as occurring at *cis*-regulatory regions with plausible biological relevance.

Integrative analyses relate adipokine-associated CpGs to metabolic gene expression

Correlations between DNAm and expression of nearby genes (±100 kb) was tested using blood-based data from the BIOS consortium (n = 3,152; **Supplementary Table 8,9**). Of the 1,069 tested CpG-gene pairs, 21.2% were connected in this analysis (n = 227, $p_{FDR} \leq 0.05$), with the majority representing inverse relationships (71.5%) in line with previous reports[21]. Thirty-five (47.9%) adiponectin CpGs were associated with expression of 46 genes (**Fig. 4c**), and 100 (47.4%) leptin CpGs were linked to 151 genes (**Fig. 4d**). Of the identified CpG-gene pairs, almost one in six involved the nearest gene in both the adiponectin (15.2%, n = 7) and leptin (15.9%, n = 24) analyses. Additionally, DNAm at two distinct CpGs (cg11851174 and cg20544516) was associated with *SREBF1*, a key regulator of lipid homeostasis[22]. In total, there were eight genes overlapping between leptin and adiponectin analyses, and several of these were central to lipid transport (e.g. *ABCG1*)[23], biosynthesis (e.g. *DHCR24*)[24], and metabolism (e.g. *CPT1A*)[25].

Biological roles for the implicated genes were interrogated using over-representation analysis. Of 16,037 gene sets tested, 79 were enriched in the 46 genes linked to adiponectin DNAm, and 15 were enriched in the 151 leptin genes (**Supplementary Table 10,11**). Findings for both adipokines highlighted links with lipid metabolism (e.g. *cholesterol metabolism* and *metabolism of lipids*). Almost half (n = 7, 46.7%) of the leptin gene sets contained the words terms *metabolic* or *metabolism*, but this pattern was reduced in the adiponectin-related terms (n = 10, 12.7%). Adiponectin gene sets were more closely linked to cellular reprogramming, including via AMPK (p_{FDR} = 3.4e−3) and mTORC1 (p_{FDR} = 9.7e−3) signalling. Overall, these pathway-level results highlighted importance for identified genes in metabolic molecular processes and regulation.

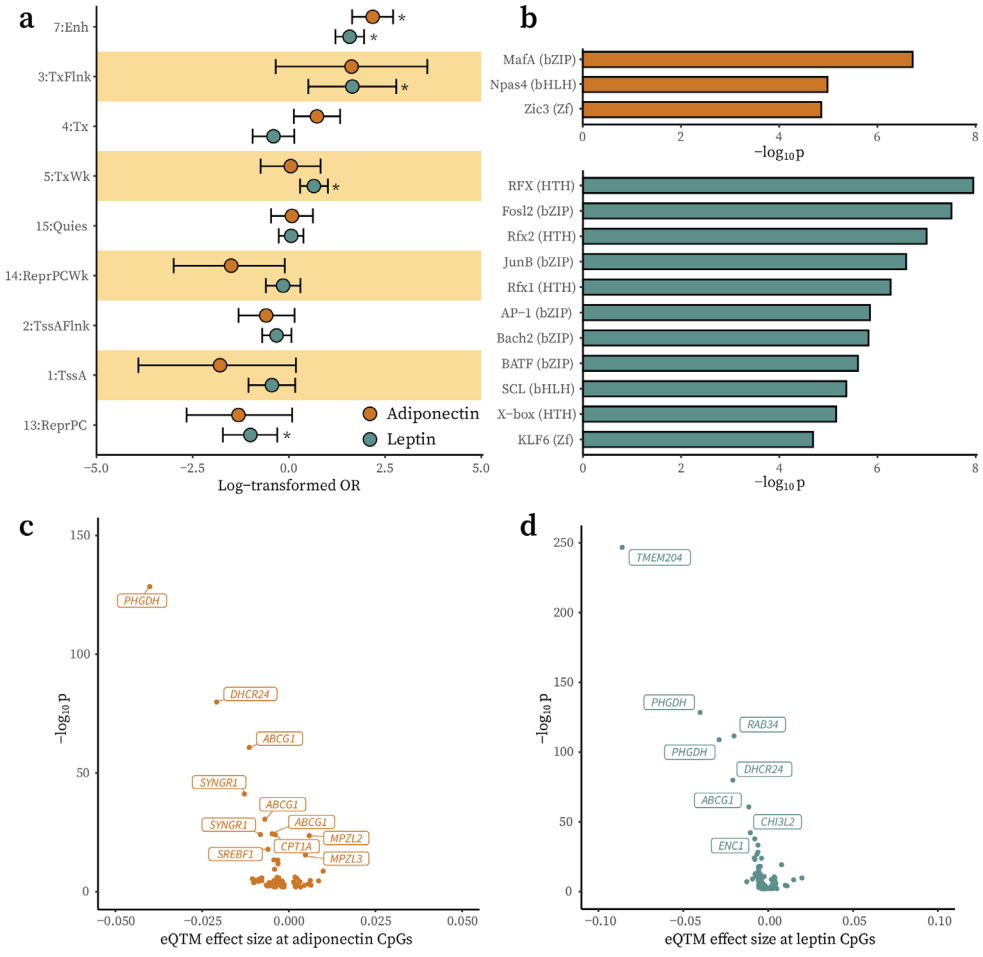

Figure 4 | Regulatory enrichment and integrative analysis results. a) Forest plot of chromatin state enrichments in adiponectin (orange) and leptin (blue) associated CpGs, identified using the PBMC Roadmap reference epigenome (E062). Natural log-transformed ORs and 95% CIs are shown. Six states with very large CIs for one or both adipokines are not shown (12_EnhBiv, 11_BivFlnk, 10_TssBiv, 9_Het, 8_ZNF/Rpts and 6_EnhG). Stars indicate significance at the 5% level after adjusting for multiple testing. **b)** Bar plot showing enriched TFBS motifs and -$\log_{10}$ *p*-values for adiponectin (orange) and leptin (blue) associated CpGs. Regions within 50bp of the CpG sites were scanned using HOMER and compared to a GC-matched random genomic background. All TFBS shown are significant at the 5% level. **c)** Volcano plot of the relationships between expression quantitative trait methylation (eQTM) effect sizes and -$\log_{10}$ *p*-values. DNAm at the adiponectin-associated CpGs and normalised expression levels of genes within 100 kb was investigated in the BIOS consortium. **d)** Volcano plot of the relationships between eQTM effect sizes and -$\log_{10}$ *p*-values for leptin-associated CpGs.

Causal inference supports DNA methylation as driving adiponectin production

Ascertaining the directionality of relationships in EWAS is far from straightforward. To shine light on the most plausible sequence of events, genetic variants were used as proxies for adipokine and DNAm exposures. In line with previous EWAS reporting, we performed bidirectional 2SMR followed by triangulation analysis[5,26]. 2SMR predicts the causal effect of an exposure on an outcome by combining genetically-determined levels of both, using GWAS or quantitative trait loci (QTL) databases. Triangulation expands upon these directional inferences and assumes that, if genetically-determined outcome levels (*observed effects*) are driven by an exposure, then they can be predicted by combining genetically-determined exposure and exposure–outcome associations (the *predicted effects*). The correlation between *observed* and *predicted effects* then quantifies the combined support for a causal direction, even if there is insufficient power at the individual CpG level. By performing both analyses bidirectionally, we comparatively inferred which direction of effect was most strongly supported by the data.

Previous EWAS have frequently concluded that blood-based DNAm is a consequence rather than a cause of investigated traits[5,8,26,27]. Therefore, we explored whether adipokine levels could be driving DNAm at identified CpGs. 2SMR did not suggest that methylation was caused by either adiponectin or leptin, and triangulation consolidated this finding with minimal correlations between *observed* (PGS-DNAm) and *predicted* (PGS-adipokine/adipokine-DNAm) effects ($R < 0.02$; **Fig. 5a,b**). In the reverse direction, 2SMR supported DNAm at two CpGs influencing adiponectin levels. The first, cg11851174 (chr17:17712609), was associated with incident T2D[26] and annotated to active chromatin in both PBMCs (4:Tx) and adipocytes (7:Enh). In the blood-based integrative analyses, this site was linked to *SREBF1* ($\beta = -0.004$, $p_{FDR} = 8.3e{-}5$), which encodes a TF central to lipid homeostasis and biosynthesis and whose expression is decreased in obesity and T2D[28].

The second CpG that putatively drove adiponectin production (cg02235049, chr3:186559186), was a novel site not previously identified in EWAS but strikingly annotated to *ADIPOQ*, the gene encoding adiponectin. Integrative follow-up into its methylation and nearby *ADIPOQ* expression was hindered in the BIOS consortium as adiponectin is not produced by immune cells. However, in publicly available DNAm and expression data from SGBS pre-adipocytes ($n = 38$), this CpG was negatively correlated with *ADIPOQ* expression ($R = -0.36$, $p = 0.029$) expression. This inverse relationship aligned with 2SMR results ($\beta = -0.217$, $p_{FDR} = 2.1e{-}12$) and a functionally repressive effect of DNAm on *ADIPOQ* expression at this adipocyte-specific enhancer.

The 2SMR direction of effect at both CpGs, where DNAm influences adiponectin, was also supported by triangulation analysis (**Fig. 5c,d**), with *observed* and *predicted effects* correlated for adiponectin ($R = 0.335$, $p = 0.030$) but not for leptin ($R = -0.017$, $p = 0.837$).

Taken together, these findings indicated a cell-type specific effect for the two CpGs identified as putative drivers of adiponectin, with evidence of links to expression for cg02235049 and cg11851174 in adipocytes and leukocytes, respectively.

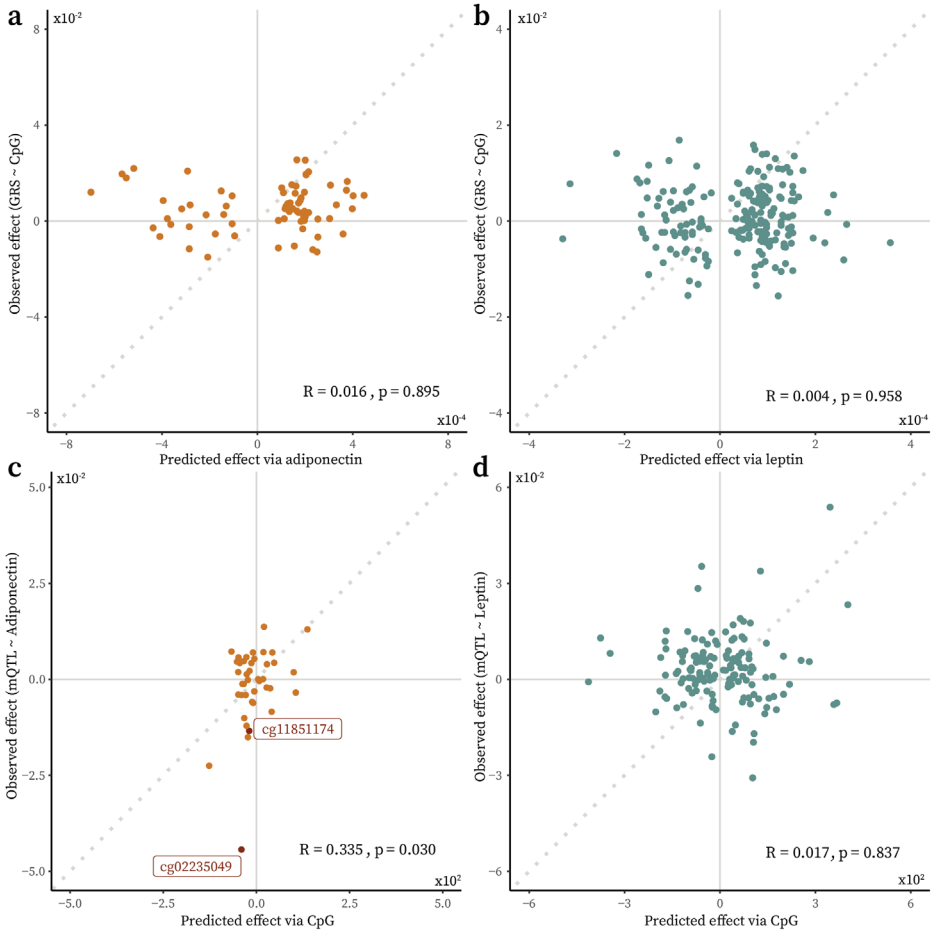

Figure 5 | Triangulation analysis results showing correlations between *predicted* (through an exposure) and *observed* genetic effects on an outcome. Pearson correlation coefficients and their associated *p*-values are shown. **a)** *Predicted* (via adiponectin) and *observed* (PGS-CpG associations) effects for the influence of genetically-determined adiponectin on DNAm at adiponectin-associated CpGs. **b)** *Predicted* (via leptin) and *observed* (PGS-CpG associations) effects for the influence of genetically determined leptin on DNAm at the leptin-associated CpGs. **c)** *Predicted* (via DNAm) and *observed* (mQTL-adiponectin) effects for the influence of DNAm at the adiponectin-associated CpGs on serum adiponectin. Two CpGs significant from the 2SMR analysis are labelled in red. **d)** *Predicted* (via DNAm) and *observed* (mQTL-leptin) effects for the influence of DNAm at the leptin-associated CpGs on leptin.

DNAm influencing adiponectin is also upstream of metabolic risk and disease

Evidence that these two CpGs (cg11851174 and cg02235049) were more likely a cause than a consequence of adiponectin combined with their links to nearby expression in relevant cell -types (*SREBF1* in blood and *ADIPOQ* in adipocytes, respectively; **Fig. 6a**), prompted deeper analysis into their clinical significance. In particular, for the *SREBF1* CpG (cg11851174) there were multiple lines of evidence pointing towards functional regulation, including previous EWAS, genomic annotation, integrative links, and causal inference (**Fig. 6b**).

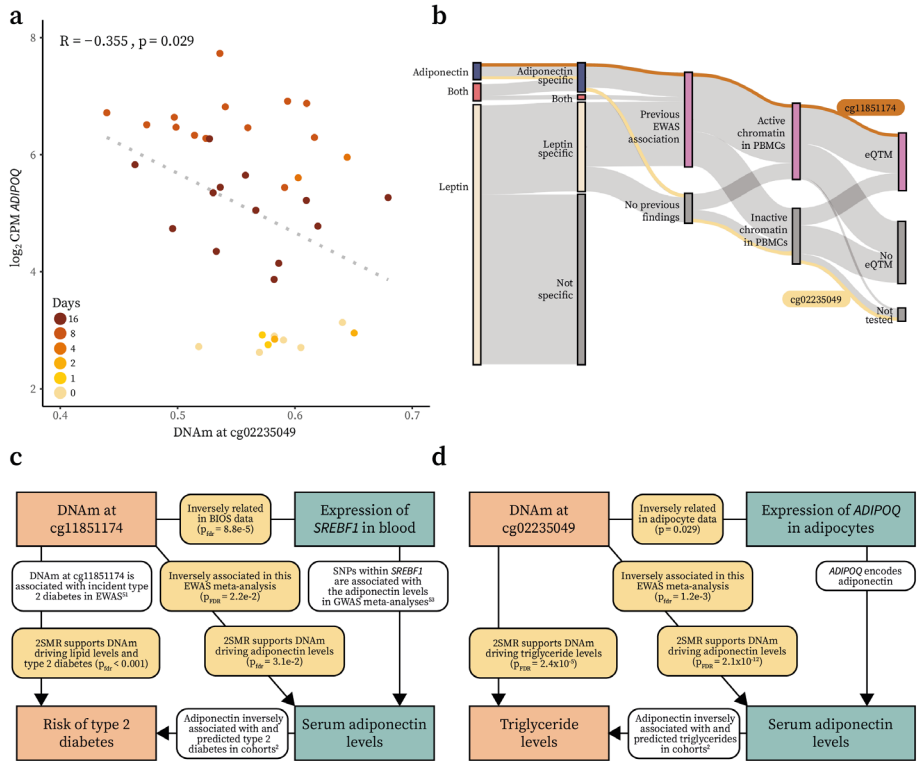

Figure 6 | Combined evidence that DNAm at two loci influences metabolic health. a) Scatter plot of DNAm at cg02235049 and normalised *ADIPOQ* expression levels in SGBS preadipocytes (n = 38). Pearson correlation coefficients and a line of best fit is shown. **b)** Sankey diagram showing multiple downstream investigations into adipokine-associated CpGs. cg11851174 is shown as having evidence supporting its functional relevance in all of these investigations (orange), and cg02235049 is shown as not having such collective evidence (yellow). **c)** Flowchart outlining the evidence linking DNAm at cg11851174 to T2D via *SREBF1* and adiponectin: findings from the current study (yellow); increases in traits (DNAm and T2D risk; orange); decreased traits (*SREBF1* expression and adiponectin; blue); and evidence from previous work (white). **d)** Flowchart showing evidence linking DNAm at cg02235049 to triglyceride levels via *ADIPOQ* and serum adiponectin.

Using 2SMR, we evaluated causal links between these two CpGs, T2D and several metabolic risk factors including fasting insulin and lipid levels. Methylation of the *SREBF1* CpG (cg11851174) plausibly decreased HDL-cholesterol levels (p_{FDR} = 4.11e−3) and increased both fasting insulin (p_{FDR} = 3.84e−3) and T2D risk (p_{FDR} = 2.39e−5). Additionally, both the *SREBF1* and *ADIPOQ* CpGs likely drove triglyceride level increases (p_{FDR} = 2.94e−2 and p_{FDR} = 2.39e−5 for cg11851174 and cg02235049, respectively). In the reverse direction, there was insufficient evidence for DNAm at either CpG responding to investigated metabolic traits or T2D itself. These results showcased these specific loci as upstream epigenetic markers of both adiponectin production and T2D pathogenesis. Coupled with evidence that *SREBF1* expression decreases T2D risk by increasing serum adiponectin[28-30] and the clear relevance of *ADIPOQ* as the gene encoding adiponectin, there is now considerable support for direct regulatory potential at these two loci in human health and metabolic risk (**Fig. 6c,d**).

Discussion

In this study, we performed an EWAS of associations between circulating adipokines and genome-wide DNAm in five blood-based cohorts (adiponectin n = 2,791; leptin n = 3,661). Through sensitivity analyses for cell-type proportions, smoking and BMI, we derived two sets of CpGs robustly associated with adiponectin (n = 73) and leptin (n = 211). Methylation at these CpGs was associated with both T2D and metabolic risk factors, including BMI, fasting insulin and HDL-cholesterol. Additionally, integrative analyses linked adipokine-associated DNAm to expression of genes central to lipid transport (e.g. *ABCG1*)[23], biosynthesis (e.g. *DHCR24*)[24], and metabolism (e.g. *CPT1A*)[25].

Bidirectional 2SMR and triangulation did not indicate a causal relationship between DNAm and leptin in either direction, but did support two CpGs as potentially regulating adiponectin production. The first of these was a novel CpG not previously identified in blood-based EWAS. Annotated to *ADIPOQ*, the gene encoding adiponectin, this CpG lies in a repressed chromatin region in PBMCs, making functional relevance for its methylation in leukocytes unlikely. Indeed, *ADIPOQ* was not expressed in the blood-based BIOS consortium data precluding integrative follow-up of this site in blood. Still, functional genomics data revealed that this CpG resided in an adipocyte-specific enhancer and, since adipocytes are the primary producers of adiponectin, this represented a biologically plausible cell-type specific effect. We therefore investigated the relationship between this CpG and *ADIPOQ* expression in adipocyte data and observed a significant, inverse correlation that aligned with our causal inference results.

This discovery underscores the potential for blood-based epigenetic analyses in large-scale cohorts to identify biologically relevant sites, even where their functional roles may be in less accessible tissues. Such associations could be driven by shared upstream factors, such as diet, causing DNAm in a tissue-agnostic manner. Although these CpGs may only be functional in some tissues (e.g. adipose), their ability to be detected in blood allows well-powered EWAS such as this one to identify biologically meaningful correlations. These sites, and others like them, will ideally serve as focal points for targeted hypothesis-driven investigations into adiponectin production by, for example, experimentally modifying methylation in adipocytes.

The second CpG plausibly driving serum adiponectin levels (cg11851174) resides in active chromatin in both PBMCs and adipocytes close to the *SREBF1* gene, which encodes a TF central to lipid homeostasis that binds to sterol regulatory elements in the promoters of genes including *ADIPOQ*[22,30]. Therefore, similar to the *ADIPOQ* CpG, this *SREBF1* site could represent a functional epigenetic effect in adipocytes being mirrored in blood. However, as we also linked increased DNAm at this site to decreased *SREBF1* expression in the large-scale blood-based BIOS consortium data, there is another plausible explanation for how DNAm could act upstream of adiponectin production. Previous experimental evidence from macrophage-specific sterol regulatory

element-binding protein (SREBP) cleavage-associating protein (SCAP) knockout mice has demonstrated that reduced SREBP-1a activity promotes macrophage polarisation to proinflammatory subtypes[31]. Therefore, circulating monocytes epigenetically primed for lower *SREBF1* expression, could feasibly have proinflammatory cell fates as adipose-tissue macrophages. Since local inflammation is an established inhibitor of adiponectin production from adipocytes, this represents a sequence of events where immune cell DNAm could more directly influence adipokine production[32]. These two hypotheses could be tested in differentiating monocytes or macrophage-adipocyte co-cultures, and our findings offer an indication of plausible mechanisms to follow-up.

Considering the collective evidence at the *ADIPOQ* and *SREBF1* loci, we investigated broader implications of these sites for metabolic disease using bidirectional 2SMR. This indicated that these CpGs may also act upstream of metabolic traits, including triglyceride levels and T2D. These directional associations, coupled with previous work implicating *SREBF1* in T2D risk via adiponectin[28-30] and the plausible relevance of *ADIPOQ* for adiponectin, reinforce these CpGs as promising sites of epigenetic control.

There were limitations to our study. Notably, we explored relationships between leukocyte DNAm and serum adiponectin with only minimal follow-up in adipocytes. Additionally, we did not adjust for smoking in our main analysis due to incomplete data, and instead opted to ensure smoking-independent effects via a two-step sensitivity analysis restricted to the subset with complete data. While sex was included as a covariate to adjust for potential confounding, no sex-stratified analyses were performed. Future research could explore whether these findings apply equally across sex and gender groups. This study was also conducted in European populations, and it remains to be tested whether our findings can be generalised to other ethnicities. Lastly, this study was not immune to the common weaknesses of molecular 2SMR. For the adipokine-DNAm 2SMR, data was not available to test all CpGs, meaning that only 57.5% of the adiponectin-associated CpGs and 61.6% of the leptin-associated CpGs were followed up in this analysis, and not all independent SNPs were available in the mQTL and GWAS datasets. This limited, and could have biased, instruments used for these exposures. In addition, most mQTLs with strong effects lie in close proximity to each other and are highly correlated. Only between one and four independent mQTLs existed to instrument each CpG and this 2SMR approach was expected to have limited success in identifying directional effects with bias towards the null[34].

In summary, this study highlights the potential of integrative, epigenome-wide studies to uncover biologically coherent epigenetic markers of molecular and metabolic traits, and reveals novel insights into the regulatory mechanisms underlying adiponectin production. By highlighting critical loci, we offer focal points for future experimental research aiming to dissect the secretory profiles of adipocytes or to identify therapeutic targets in metabolic disease.

Methods

Cohort descriptions

Leiden Longevity Study (LLS) The LLS is a cohort of long-lived, Dutch, Caucasian siblings (*n* = 944), who were recruited with their offspring (*n* = 1,671) and their offspring's partners (*n* = 744)[35]. Between 2002 and 2006, research nurses collected non-fasted blood samples from living study participants for isolation of DNA, RNA, serum, and plasma, and these were stored at -80˚C until analysis. From these samples, adiponectin levels were determined with the DuoSet ELISA kit (R&D Systems Europe Ltd, Abingdon, United Kingdom) according to the manufacturer's instructions. The lower and upper detection limits of the assay were respectively 62.5 and 4000 pg/ml. Serum leptin was measured using 'two-step' sandwich ELISA kit (Diagnostics Biochem Canada Inc., Dorchester, Ontario, Canada) according to manufacturer's instructions. Assay sensitivity was 0.5 ng/ml.

DNAm data of whole blood samples was generated from 821 unrelated participants from the offspring-partner generation of the LLS by the Human Genotyping facility (HuGe-F, Erasmus MC, Rotterdam, The Netherlands) within the Biobank-Based Integrative Omics Studies (BIOS) consortium, funded by BBMRI-NL, a research infrastructure financed by the Dutch government (NWO 184.021.007). Genomic DNA (500ng) was bisulfite converted using the Zymo EZ-96 DNA methylation kit (Zymo Research Corp, Irvine, CA, USA). 4 µl was then hybridized on the Infinium HumanMethylation450 BeadChip array (Illumina Inc, San Diego, CA, USA) according to the manufacturer's protocol. Data preprocessing and quality control followed the *DNAmArray* workflow[36].

Kooperative Gesundheitsforschung in der Region Augsburg (KORA) The KORA F4 study (2006-2008) followed up individuals (*n* = 3,080) living in the region of Augsburg, Southern Germany, aged between 32 and 81 years old[37]. Blood samples were drawn after an 8 hour fast and frozen at -80˚C until analysis. Serum leptin concentrations were determined using ELISAs from Mecodia, Stockholm, Sweden. The intra- and inter-assay coefficients of variation for leptin were <10%. Serum adiponectin levels were measured in the subsample aged 61 to 82 years using the Quantikine ELISA kit from R&D Systems (Wiesbaden, Germany)[38]. The intra- and inter- assay coefficients of variation were 3.8% and 8.0%, respectively.

Following isolation according to standard procedures, genomic DNA (750 ng) from 1,707 whole blood samples was bisulfite converted with the Zymo EZ-96 DNA Methylation Kit (Zymo Research Corp, Irvine, CA, USA). 4 µl from each sample underwent amplification, enzymatic fragmentation, and application to the Infinium HumanMethylation450 BeadChip array (Illumina Inc, San Diego, CA, USA) according to the manufacturer's protocol[39]. GenomeStudio with the methylation module was used to extract and process the raw image data and initial quality assessment was conducted using the Control Dashboard. For data pre-processing, a common pipeline was used[40].

TwinsUK Fasting morning serum total adiponectin levels were measured with a two-site DELFIA assay using antibodies and standards from R&D Systems (Minneapolis, MN). The day-to-day coefficient of variation (CV) for adiponectin was 9.9% at a concentration of 3.2 ng/ml, 7.8% at 8.6 ng/ml, and 5.2% at 14.7 ng/ml. Serum leptin concentration was determined after an overnight fast using an RIA (Linco Research, St. Louis, MO).

As described previously, fasting whole blood DNAm of individuals in TwinsUK was profiled using the Infinium HumanMethylation450 BeadChip (Illumina Inc, San Diego, CA)[41]. DNAm was assessed at over 450,000 sites and processing of methylation signals was performed with R Bioconductor software[42]. Briefly, the ENmix package[43] was used for quality control of the data, and the *minfi* package was used to exclude samples with median methylated and unmethylated signal ratio less than 10.5[44]. Background correction, dye bias correction, and quantile normalization were performed with ENmix as described previously[45]. Underperforming probes and outlier samples were identified using standard parameter values and signals with detection *p*-value above 1e-6 and number of beads fewer than three were excluded. Maximum probe and sample missingness were set to 5%.

The Study of Health in Pomerania (SHIP-TREND) The Study of Health in Pomerania – Trend (SHIP-TREND) is a longitudinal population-based cohort study in West Pomerania, a region in the north-east of Germany, which assesses the prevalence and incidence of common population-relevant diseases and their risk factors. Baseline examinations for SHIP-TREND were carried out between 2008 and 2012, comprising 4,420 participants aged 20 to 81 years. Study design and sampling methods were previously described[46].

DNA was extracted from blood samples (n = 508) of SHIP-TREND participants to assess DNA methylation using the Illumina HumanMethylationEPIC BeadChip array. Samples available for this project were randomly selected based on the availability of multiple OMICS data, and excluding T2D. The samples were taken between 7:00 a.m. and 4:00 p.m., and serum aliquots were prepared for immediate analysis and for storage at -80 °C in the Integrated Research Biobank (Liconic, Liechtenstein). Processing of the DNA samples was performed at the Helmholtz Zentrum München. Preparation and normalization of the array data was performed according to the CPACOR workflow[47]. The IDAT files were processed using the *minfi* package[44]. Probes that had a detection p-value above background (sum of per-array methylated and unmethylated intensity valuesbased p-value ≥ 1e-16) were set to missing. Methylation β values were calculated as proportion of methylated intensity value on the sum of methylated + unmethylated + 100 intensities. Arrays with observed technical problems (±4SD outside control probe intensity mean) during steps like bisulfite conversion, hybridization or extension, as well as arrays with mismatch between sex of the proband and sex determined by the chr X and Y probe intensities were removed from subsequent analyses. Additionally, only arrays with a call rate above 95% were processed further, resulting in 495 samples with methylation data on 865,859 sites, and 441 samples with phenotype data available for subsequent analyses. In addition to sex, age, and white blood cell type counts, the first six principal components of the control probe intensities obtained by the CPACOR workflow were included in the model as covariates to account for unmeasured confounders. Details on assessment of the metabolic phenotypes and covariates used in this analysis are provided within the SHIP cohort design publication[46].

LifeLines DEEP (LLD) A total of 701 adults from the Lifelines DEEP cohort were included in this study based on available methylation data and cytokines. Initially, 1539 participants were enrolled in the Lifelines DEEP, which is a subpopulation of the Lifelines cohort in the north of The Netherlands[48,49]. Except for the regular Lifelines procedures, additional deep molecular measurements were performed in Lifelines DEEP participants. The plasma levels of leptin (ng/ml) and adiponectin (µg/ml) were measured by enzyme-linked immunosorbent assay (ELISA) platform.

For genome-wide DNA methylation data, 500 ng of genomic DNA was bisulfite-converted using the EZ DNA Methylation kit (Zymo Research Corp., USA) and hybridized on Illumina HumanMethylation450 BeadChip arrays (Illumina, Inc.) according to the manufacturer's protocols. The original IDAT files were generated by the Illumina iScan BeadChip scanner and performed by the Human Genotyping facility (HugeF) of ErasmusMC, The Netherlands (http://www.glimDNA.org/). Quality control and normalization details are described elsewhere[50]. Methylation levels at each CpG site were expressed as the ratios of the methylated intensity over the total intensity (β-values), which were used for the subsequent statistical analyses.

Cohort-based analyses

Main analysis All contacted cohorts with sufficient data followed a common analysis plan, and all samples analysed were from distinct individuals (i.e. there were no repeat measurements included in the analysis). DNAm was measured either by the Illumina Infinium HumanMethylation450 (in LLS, KORA, TwinsUK, and LLD cohorts) or MethylationEPIC BeadChip array (in SHIP-TREND cohort). Adipokine measurements below the limit of detection and outlying values for DNAm, adiponectin and leptin (more than three IQRs from the nearest quartile) were removed prior to analysis. Cell-type proportions were predicted from DNAm data using the IDOL algorithm[51].

For each of *j* CpGs measured in *i* individuals, a linear regression model (see Equation 1 for general specification) was fitted of DNAm β values on natural log-transformed adiponectin (μg/ml) or leptin (ng/ml). All models were adjusted for age (in years), sex, cell-type proportions predicted from DNAm data (monocytes, CD8+ T cells, CD4+ T cells, natural killer (NK) cells and B cells) and technical covariates (left to the analyst's discretion). Sex was considered in the study design and included as a covariate in statistical models to address potential biological differences. Analyses were not stratified by sex, and gender identity was not recorded.

$$DNAm_{\beta_{ij}} = \beta_0 + \beta_1 \cdot ln(adipokine)_i + \beta_2 \cdot age_i + \beta_3 \cdot sexFemale_i + \beta_4 \cdot CD8T_i + \beta_5 \cdot CD4T_i + \beta_6 \cdot NK_i + \beta_7 \cdot Mono_i + \beta_8 \cdot technical\_factors_i \quad [1]$$

Sensitivity analyses Effects of adjustment for smoking status on the relationship between adipokines and identified CpGs was investigated in a sensitivity analysis, where each cohort added trichotomous smoking to the cohort-specific base models as a categorical fixed effect. In some cases, this resulted in a reduction of the sample size as there was missingness in the smoking data. To distinguish BMI-independent signals, cohorts also ran an additional analysis adjusting for BMI (measured in kg/m^2).

All cohorts also investigated the effect of adjusting for extended cell types, estimated using the epiDISH Bioconductor package release 3.20, which became available in the timeframe of this project[52]. Basophils, memory B cells, naive B cells, CD4+ memory T cells, CD4+ naive T cells, CD8+ memory T cells, CD8+ naive T cells, eosinophils, monocytes, NK cells and regulatory T cells were added to the base model for all cohorts. Neutrophils were excluded to avoid collinearity as proportions for all cells sum to 1.

Meta-analyses

Differentially methylated probes Results from each cohort were inspected and rows were removed if they were estimated from fewer than 50 observations. Probes located on sex chromosomes, in ENCODE Blacklist regions[53], or that contained common genetic variants or that were ambiguously mapped[54] were also removed. To ensure good quality data, we inspected QQ, volcano and Manhattan plots, alongside boxplots of the effect size and SE distributions across cohorts. Following these steps, data were available on 412,224 CpGs from the base adiponectin model and 406,832 CpGs for the base leptin model.

The Bioconductor package *bacon* estimated and adjusted for bias and inflation of the test statistics, using default priors (α = 1.28, β = 0.36)[55]. After running bacon, inflation and bias were estimated at ~1.00 and within ±0.00 for all models, respectively. Bacon-adjusted effect sizes and SEs were used as input in a fixed-effects meta-analysis in *METAL* version 2011-03-25[56]. Separate analyses were performed for each of the base models and each extended model (adjusted for smoking, BMI and extended cell counts). Any CpGs for which there was evidence of high heterogeneity in effect sizes between cohorts ($I^2 \geq 80\%$) would have been removed but there were none. CpGs were regarded as significantly associated with the relevant adipokine if the false discovery rate (FDR)-adjusted *p* value was below 0.05, and only CpGs that still met this criterion in the additional sensitivity analyses for smoking, cell-type proportions and BMI were taken forward into downstream analyses.

Differentially methylated regions To assess distinct genomic loci associated with circulating adipokine levels, differentially methylated regions (DMRs) were identified using the *DMRfinder* algorithm[57], as implemented in the *DNAmArray* workflow version 2.1[36]. DMRs were defined as regions with at least three differentially methylated positions (DMPs) and an inter-CpG distance of less than 1 kb, allowing a maximum of three non-DMPs across a DMR. The number of distinct loci was calculated as the total number of DMPs minus the number of DMPs in DMRs plus the number of DMRs called by *DMRfinder*.

Functional annotation

Phenotype enrichment Using summary data from the EWAS catalogue[58] and EWAS atlas[59], our CpGs were investigated for previous associations with other phenotypes. Any EWAS meeting the following criteria was removed: without an associated PubMed ID; with a sample size under 500; that reported fewer than 100 CpGs in the respective database; missing nominal *p* values; not performed in adults; or not using whole blood or leukocyte samples. Traits were also recoded to ensure consistency between names, for example by combining EWAS of 'BMI' and 'body mass index'. This resulted in a list of 57 traits, which were tested for enrichment of associations with our CpGs using logistic regression.

Chromatin state enrichment Identified CpGs were annotated to chromatin state using immune cell and adipocyte Roadmap reference epigenomes[13]. Logistic regression models were fitted using the *glm* function in R to calculate and test ORs for each of the 15 chromatin states. Nominal p-values were adjusted for multiple testing using FDR and enrichments or depletions were assessed at a 5% significance threshold.

Transcription factor binding site (TFBS) enrichment A 50 bp window around identified CpGs was scanned using *findMotifsGenome.pl* from HOMER version 3.1 for enrichment of known motifs compared with a random genomic background matched for GC content[60]. ENCODE TFBS annotation for TFs and CpGs on the 450k array was used to further investigate the size of binding sites and distance from CpG to summit[54]. TFs associated with enriched TFBS were examined for links with metabolic health and, specifically, adiponectin and leptin pathways and interactions.

eQTM analyses Measurements of blood-based gene expression alongside DNAm from the same samples was available from the BIOS consortium (n = 3152). This dataset comprises six Dutch biobanks: the Cohort on Diabetes and Atherosclerosis Maastricht[61], LifeLines[48], LLS[35], Netherlands Twin Register[62,63], Rotterdam Study[64], and the Prospective ALS Study Netherlands[65]. After filtering out non-autosomal and lowly expressed genes, count data were transformed into $\log_2$ counts per million (CPM) using *edgeR*, and values for each gene were rank inverse normal (RIN)-transformed prior to analysis[66].

Genomic locations of human transcripts, exons, coding sequences and genes were imported from the Ensembl database using *makeTxDbFromEnsembl* from the GenomicFeatures Bioconductor package[67]. These were used to identify the nearest gene to each adipokine-associated CpG and to save a list of all genes within 100 kb of each CpG. To examine links between DNAm and gene expression, linear regression models were fitted with RIN-transformed $\log_2$CPM values as the response variable and methylation β values as the independent variable, adjusting for the effects of age, sex, technical covariates (row, plate, and flowcell) and twelve blood-cell counts predicted from DNAm using EpiDISH release 3.20[52].

For investigations into links between expression and DNAm in Simpson-Golabi-Behmel syndrome (SGBS) pre-adipocytes, publicly available data were downloaded from Gene Expression Omnibus (GEO) using GEOquery in R release 3.20. Data were available for the same samples, with expression profiled using the Illumina HumanHT-12 V4.0 expression BeadChip microarray and DNAm profiled using the Illumina Infinium HumanMethylation450 BeadChip array[68]. Count data were normalised to $\log_2$CPM values and values from probes interrogating *ADIPOQ* (ILMN_1775045) and *SREBF1* (ILMN_1663035, ILMN_1695378 and ILMN_2328986) were extracted. Additionally, β values from cg11851174 and cg02235049 were subset from the DNAm data. Complete information was available for 38 samples across five timepoints (days 0, 1, 2, 4, 8 and 16). Expression and DNAm values were plotted against one another for the relevant comparisons and correlation coefficients were calculated.

Over-representation analysis On the basis of the large-scale blood-based integrative analysis in BIOS, a list of CpGs for which there was evidence for epigenetic regulation of nearby gene expression in leukocytes was saved. The associated gene names were used as input for over-representation analysis using 11 recent (updated in the last 6 years) databases relating to human health and disease downloaded from *Enrichr* (BioPlanet 2019, Elsevier Pathway Collection, GeDiPNet 2023, GO Biological Process 2023, KEGG Human 2021, MSigDB Hallmark 2020, OMIM, PhenGenI Association 2021, PheWeb 2019, Reactome 2022 and WikiPathway Human 2021). These databases were imported into R and analyses were performed using the *Enrichr* function from clusterProfiler release 3.20[69]. *p*-values were FDR-adjusted for multiple testing and significance was assessed at the 5% level.

Causal inference

Two-sample Mendelian Randomization To assess the direction of effects between adipokines and DNAm at identified CpGs, the *TwoSampleMR* package was used to perform bidirectional 2SMR[70]. This instrumental variable (IV)-based method uses genome-wide association study (GWAS) summary statistics to infer whether a risk factor causally influences an outcome. 2SMR relies on several key assumptions, namely that instruments are relevant, independent and that there is no horizontal pleiotropy. To interrogate the effects of DNAm at our CpGs on adiponectin and leptin, we extracted *cis*-methylation quantitative trait locus (mQTL) data from the Genetics of DNA Methylation Consortium (GoDMC)[71] and combined these with summary statistics from recent, large-scale GWAS of both adiponectin[72] and leptin[73]. For some CpGs (42.5% for adiponectin and 38.4% for leptin), there was insufficient data available to interrogate the effects of DNAm at that CpG. For the remaining CpGs, between one and four independent SNPs with data on both their *cis*-association with DNAm and association with the relevant adipokine were used as instruments. These were combined using the Wald ratio (for single mQTL instruments) or inverse variance weighted (IVW) methods (for multiple, independent mQTLs).

To interrogate the influence of adipokine levels on DNAm at identified CpGs, independent GWAS variants from recent, large-scale analyses were used[72,73]. Of the 18 variants that could instrument adiponectin, there were *trans*-mQTL data in GoDMC available for four of them and, of the six variants that could instrument leptin, there was available data for one. Linkage disequilibrium (LD) proxies with $R^2 > 0.8$ for the remaining SNPs were downloaded from the NIH's LDlink tool[74], and GoDMC data[71] were extracted for these where available. This process identified two other instrumental SNPs that could instrument the adipokines, one for each, meaning that leptin was instrumented by two independent SNPs (rs8043757 and rs4665972) and adiponectin was instrumented by five independent SNPs (rs11023332, rs1108842, rs12051272, rs998584 and rs113086489). The GWAS summary statistics and mQTL effects were then combined using the IVW method and the *TwoSampleMR* package in R version 0.6.6. For all analyses, *p*-values were adjusted for multiple testing using the FDR method and potential causal effects were assessed at the 5% significance threshold.

The following cohorts were used to derive both mQTL effects in GoDMC and adiponectin and/or leptin GWAS effects and therefore had overlapping individuals in both the exposure and outcome datasets for the 2SMR analysis: Rotterdam Study (GoDMC 1472 samples, leptin GWAS 3932 samples); and TwinsUK (GoDMC 843 samples, adiponectin GWAS 968 and 1229 samples, leptin GWAS 5654 samples). Overall, the overlap was low considering that all three meta-analyses incorporated data from over 16 cohorts.

The *TwoSampleMR* package version 0.6.6 was also used to interrogate causal links between DNAm at CpGs and metabolic traits. CpGs were instrumented with independent *cis*-mQTLs obtained from GoDMC, and *ieugwasr* was used to extract MR instruments for the metabolic traits. Reference numbers for the investigated traits were as follows: type 2 diabetes (ebi-a-GCST006967); fasting insulin (ebi-a-GCST9002238); triglycerides (ieu-b-111); HDL-cholesterol (ieu-b-109); and BMI (ieu-b-40).

Triangulation analyses To perform triangulation analyses, we interrogated the correlation between the *observed effect* of an IV on an outcome (i.e. mQTL–adipokine or polygenic score (PGS)–DNAm associations) and the predicted effect via the exposure. This analysis assumes that if the effect of an exposure on an outcome is causal, it would be possible to predict the IV's effect on the outcome through a combination of its effect on the exposure and the exposure's association with the outcome (the *predicted effect*).

In detail, when looking at the effect of DNAm on adipokine levels (consequential analysis), the *observed effect* is the association between the top mQTL and ln(adipokine), extracted from the full GWAS summary data. The *predicted effect* combines mQTL and EWAS statistics to estimate the influence of an additional effect allele (EA) on the outcome (i.e. the adipokine). For each additional EA, the expected rise in DNAm at the CpG is equivalent to the mQTL effect size (β_{mQTL}). As the EWAS effect size represents the DNAm effect associated with a one-unit increase in the adipokine level, the expected increase in the adipokine level for a β_{mQTL} increase in DNAm can be calculated as the product of the mQTL and EWAS effects (i.e. $\beta_{mQTL} \times \beta_{EWAS}$). SNP effects on DNAm (mQTL effects) were extracted from GoDMC data[35] and CpG-adipokine effects were extracted from the EWAS meta-analysis presented here.

When looking in the reverse direction (i.e. adipokines as a cause of DNAm), the *observed effect* is a PGS, where the influence of adipokine-associated SNPs on DNAm are weighted by their EA frequency (EAF). The *predicted effect* here uses equivalent EAF weighting and is calculated as PGS~adipokine/adipokine~CpG. The observed and predicted effects in both directions were visualised using scatter plots and correlation was assessed with Pearson correlation coefficients.

Ethics statement

Leiden Longevity Study (LLS) Written informed consent for DNA collection and its use for genetic analyses was obtained from all participants prior to their enrolment into the study. Good clinical practice guidelines were maintained, and the study protocol was approved by the local Medical Ethical Committee of the Leiden University Medical Center.

Kooperative Gesundheitsforschung in der Region Augsburg (KORA) In accordance with the Declaration of Helsinki, written informed consent was obtained from all participants prior to their enrolment into the study. Good clinical practice guidelines were maintained, and the study protocol was approved by the Ethics Committee of the Bavarian Medical Association.

TwinsUK Ethical approval was initially granted by the St. Thomas' Hospital Research Ethics Committee, with subsequent approvals overseen by the NRES Committee London - Westminster following restructuring. In September 2007, ongoing approval was granted, ensuring indefinite continuation.

SHIP-TREND The medical ethics committee of the University of Greifswald approved the study protocol, and oral and written informed consents were obtained from each of the study participants.

LifeLines DEEP (LLD) All participants provided written informed consent. The Lifelines DEEP study was approved by the Medical Ethical Committee of the University Medical Center Groningen (UMCG), Groningen, The Netherlands

Author contributions

L.S. conceived and designed the study, performed data preprocessing and quality control, undertook cohort-specific and main analyses, interpreted results and drafted the manuscript. B.T.H. conceived and designed the study, supervised conduct of the study, iteratively critically revised the manuscript and provided critical intellectual contributions and interpretations of results. T.D. and R.W.

(KORA F4), X.L. (LLD), Y.X. and R.C. (TwinsUK) and M.K.N. (SHIP-TREND) performed cohort specific analyses, provided summary statistics for the meta-analyses, and provided critical intellectual contributions and interpretations of results; J.M.O. provided critical intellectual contributions and interpretations interpretations of results. L.F., A.Z., J.F. and H.S. (LLD), C.G., C.H., W.K., A.P. and M.W. (KORA F4), M.D., H.J.G., M.N. and A.T. (SHIP-TREND), J.T.B. (TwinsUK), and M.B. and P.S. (LLS) provided data, phenotype acquisition and harmonisation for these analyses, and provided critical intellectual contributions and interpretation of results. All authors reviewed the manuscript and approved the final version.

Funding

The work of L.S. was supported by the Joint Programming Initiative 'a Healthy Diet for a Healthy Life' (JPI-HDHL) DIMENSION project [ZonMW project number: 529051021]. Funding for the BIOS consortium was provided by the Netherlands Organization for Scientific Research (NWO 184.021.007 and 184.033.111), made available as a Rainbow Project of the Biobanking and Biomolecular Research Infrastructure Netherlands (BBMRI-NL).

LLD The Lifelines Biobank initiative has been made possible by a subsidy from the Dutch Ministry of Health, Welfare and Sport; the Dutch Ministry of Economic Affairs, the University Medical Centre Groningen (UMCG, the Netherlands); the University of Groningen and the Northern Provinces of the Netherlands. J.F. is supported by the ERC Consolidator grant (grant agreement no. 101001678), NWO-VICI grant VI.C.202.022 and the Ammodo Science Award 2023 for Biomedical Sciences from Stichting Ammodo.

SHIP-TREND SHIP (The Study of Health in Pomerania) is part of the Community Medicine Research net of the University of Greifswald, Germany, which is funded by the Federal Ministry of Education and Research (grant no. 01ZZ9603, 01ZZ0103 and 01ZZ0403), the Ministry of Cultural Affairs as well as the Social Ministry of the Federal State of Mecklenburg-West Pomerania, and the network 'Greifswald Approach to Individualized Medicine (GANI_MED)' funded by the Federal Ministry of Education and Research (grant 03IS2061A). DNAm data have been supported by the DZHK (grant 81X3400104). A.T. has been funded by the Deutsche Forschungsgemeinschaft (DFG, German Research Foundation) - 542489987. The University of Greifswald is a member of the Caché Campus program of the InterSystems GmbH.

TwinsUK TwinsUK is funded by the Wellcome Trust, Medical Research Council, Versus Arthritis, European Union Horizon 2020, Chronic Disease Research Foundation (CDRF), Zoe Ltd. and the National Institute for Health Research (NIHR), Clinical Research Network (CRN) and Biomedical Research Centre based on Guy's and St Thomas' NHS Foundation Trust in partnership with King's College London.

KORA F4 The KORA research platform (KORA, Cooperative Health Research in the Region of Augsburg) was initiated and financed by the Helmholtz Munich – German Research Center for Environmental Health, which is funded by the German Federal Ministry of Education and Research and by the State of Bavaria. Furthermore, KORA research was supported within the Munich Center of Health Sciences (MC Health), Ludwig-Maximilians-Universität, as part of LMUinnovativ. This work was supported by the German Federal Ministry of Education and Research (BMBF) within the framework of the EU Joint Programming Initiative 'A Healthy Diet for a Healthy Life' (DIMENSION; grant no. 01EA1902A). The German Diabetes Center is supported by the Ministry of Culture and Science of the state of North-Rhine Westphalia (Düsseldorf, Germany) and the German Federal Ministry of Health (Berlin, Germany). This study was supported in part by a grant from the German Federal Ministry of Education and Research to the German Center for Diabetes Research (DZD).

LLS The LLS was supported by a grant from the Innovation-Oriented Research Program on Genomics (SenterNovem IGE01014 and IGE05007), the Centre for Medical Systems Biology, and

the National Institute for Healthy Ageing (grant 05040202 and 05060810), in the framework of the Netherlands Genomics Initiative / Netherlands Organization for Scientific Research, and the VOILA Consortium (ZonMW 457001001).

Funders had no say in the study design, collection, analysis, interpretation, or writing of this work.

Declarations of interest

H.J.G. has received travel grants and speaker's honoraria from Neuraxpharm, Servier, Indorsia and Janssen Cilag. C.H. is Reviews Editor at Diabetologia. The authors declare that there are no other relationships or activities that might bias, or be perceived to bias, their work.

Data & code availability

Individual-level data Regarding individual-level data from the cohorts involved, the informed consents given by KORA study participants does not cover data posting in public databases. However, data are available upon request from KORA Project Application Self-Service Tool (https://helmholtz-muenchen.managed-otrs.com/external/Data). Requests for data can be submitted online and are subject to approval by the KORA Board. The data of the SHIP study cannot be made publicly available due to the informed consent of the study participants but it can be accessed through a data application form available at https://transfer.ship-med.uni-greifswald.de/ for researchers who meet the criteria for access to confidential data. The HumanMethylation450 BeadChip data from the LLD and LLS are available as part of the BIOS Consortium in the European Genome-phenome Archive (EGA), under the accession code EGAD00010000887 (https://ega-archive.org/datasets/EGAD00010000887). Additional genomic and phenotype data are available upon request via the BBMRI-NL BIOS consortium. All data can be requested by bona fide researchers from the respective cohorts.

All other data used in this study is publicly available EWAS summary statistics can be downloaded from the EWAS Catalogue[58] and EWAS atlas[59], PBMC reference epigenome data are available from ROADMAP[13], TFBS data are available within the HOMER software[60], full mQTL summary statistics can be requested from GoDMC[71], adiponectin[72] and leptin[73] GWAS summary statistics are available from the GWAS database, LD proxies and matrices can be accessed using LDlink[74], variances in methylation and expression were calculated from data generated by the BIOS (a full list of investigators is available from https://ega-archive.org/datasets/EGAD00010000887), libraries for GSEA were downloaded directly from Enrichr (https://maayanlab.cloud/Enrichr/), and SGBS adipocyte data are available from GEO (GSE119593 for expression data, GSE119539 for DNAm data)[68].

Custom code availability R scripts for the respective analyses are deposited in a GitHub repository at `nebulyra/adipo_ewas`.

All software used is open source and freely available Unless stated otherwise, all calculations were performed using R version 4.2.2. For all meta-analyses, METAL, version 2011-03-25 was used[56]. TFBS enrichment analyses were performed using HOMER version 3.1[60].

Acknowledgements

The authors thank the staff, participants and related contributing research centres for all cohorts involved in this study. We are additionally grateful to P. S. DeVries (Human Genetics Center, University of Texas Health Science Center at Houston, USA) for his support with the SHIP-TREND EWAS pipeline.

References

1. Fahed, G. *et al.* Metabolic syndrome: updates on pathophysiology and management in 2021. *Int J Mol Sci* **23** (2):786 (2022).
2. Mir, M. M. *et al.* Differential association of selected adipocytokines, adiponectin, leptin, resistin, visfatin and chemerin, with the pathogenesis and progression of type 2 diabetes mellitus (T2DM) in the Asir region of Saudi Arabia: a case control study. *J Pers Med* **12** (5): 735 (2022).
3. Un Nisa, K. *and* Reza, M. I. Key relevance of epigenetic programming of adiponectin gene in pathogenesis of metabolic disorders. *Endocr Metab Immune Disord Drug Targets* **20** (4): 506-517 (2019).
4. Wróblewski, A. *et al.* Molecular insight into the interaction between epigenetics and leptin in metabolic disorders. *Nutrients* **11** (8): 1872 (2019).
5. Wielscher, M., *et al.* DNA methylation signature of chronic low-grade inflammation and its role in cardio-respiratory diseases. *Nat Commun* 13 (1): 2408 (2022).
6. Gomez-Alonso, M. D. C., *et al.* DNA methylation and lipid metabolism: an EWAS of 226 metabolic measures. *Clin Epigenetics* **13** (1): 1–19 (2021).
7. Willmer, T. *et al.* Blood-based DNA methylation biomarkers for type 2 diabetes: potential for clinical applications. *Front Endocrinol (Lausanne)* **9**: 744 (2018).
8. Dekkers, K.F. *et al.* Blood lipids influence DNA methylation in circulating cells. *Genome Biol* **17** (1): 138 (2016)
9. Davis, F. M. *and* Gallagher, K. A. Epigenetic mechanisms in monocytes/macrophages regulate inflammation in cardiometabolic and vascular disease. *Arterioscler Thromb Vasc Biol* **39** (4): 623-634 (2019).
10. Aslibekyan, S. *et al.* CPT1A methylation is associated with plasma adiponectin. *Nutr Metab Cardiovasc Dis* **27** (3) :225 (2016).
11. Suriano, F. *et al.* Novel insights into the genetically obese (ob/ob) and diabetic (db/db) mice: two sides of the same coin. *Microbiome* **9** (1): 147 (2021).
12. Matsubara, M., Maruoka, S., *and* Katayose, S. Inverse relationship between plasma adiponectin and leptin concentrations in normal-weight and obese women. *Eur J Endocrinol* **147** (2): 173-180 (2002).
13. Roadmap Epigenomics Consortium *et al.* Integrative analysis of 111 reference human epigenomes. *Nature* **518** (7539): 317-330 (2015).
14. Heintzman, N. D. *et al.* Distinct and predictive chromatin signatures of transcriptional promoters and enhancers in the human genome. *Nat Genet* **39** (3): 311-318 (2007).
15. Kaluscha, S. *et al.* Evidence that direct inhibition of transcription factor binding is the prevailing mode of gene and repeat repression by DNA methylation. *Nat Genet* **54** (12): 1895-1906 (2022).
16. Liu, G. *and* Liu, F. Bach2: a key regulator in Th2-related immune cells and Th2 immune response. *J Immunol Res* **2022**: 2814510 (2022).
17. Murphy, T. L., Tussiwand, R., *and* Murphy, K. M. Specificity through cooperation: BATF-IRF interactions control immune-regulatory networks. *Nat Rev Immunol* **13** (7): 499-509 (2013).
18. Liu, Y. *et al.* Clathrin-associated AP-1 controls termination of STING signalling. *Nature* **610** (7933): 761-767 (2022).
19. Wrann, C.D. *et al.* FOSL2 promotes leptin gene expression in human and mouse adipocytes. *J Clin Invest* **122** (3): 1010-1021 (2012).
20. Tsuchiya, M. *et al.* Suppression of MafA mRNA with siRNA prevents adipose cell differentiation in 3T3-L1 cells. *Int J Mol Med* **23** (6): 725-732 (2009).
21. Bonder, M. J. *et al.* Disease variants alter transcription factor levels and methylation of their binding sites. *Nat Genet* **49** (1): 131-138 (2017).
22. Shimano, H. *and* Sato, R. SREBP-regulated lipid metabolism: convergent physiology-divergent pathophysiology. *Nat Rev Endocrinol* **13** (12): 710-730 (2017).
23. Kennedy, M. A. *et al.* ABCG1 has a critical role in mediating cholesterol efflux to HDL and preventing cellular lipid accumulation. *Cell Metab* **1** (2): 121-131 (2005).
24. Zerenturk, E. J. *et al.* Desmosterol and DHCR24: unexpected new directions for a terminal step in cholesterol synthesis. *Prog Lipid Res* **52** (4): 666-680 (2013).
25. Schlaepfer, I. R. *and* Joshi, M. CPT1A-mediated fat oxidation, mechanisms, and therapeutic potential. *Endocrinology* **161** (2): bqz046 (2020).
26. Wahl, S. *et al.* Epigenome-wide association study of body mass index, and the adverse outcomes of adiposity. *Nature* **541** (7635): 81-86 (2017).
27. Hillary, R.F. *et al.* Blood-based epigenome-wide analyses of 19 common disease states: a longitudinal, population-based linked cohort study of 18,413 Scottish individuals. *PLoS Med* **20** (7): e1004247 (2023).
28. Harding, A. H. *et al.* Polymorphisms in the gene encoding sterol regulatory element-binding factor-1c are associated with type 2 diabetes. *Diabetologia* **49** (11): 2642-2648 (2006).
29. Felder, T. K. *et al.* The SREBF-1 locus is associated with type 2 diabetes and plasma adiponectin levels in a middle-aged Austrian population. *Int J Obes (Lond)* **31** (7): 1099-1103 (2007).

30. Seo, J.B. *et al.* Adipocyte determination- and differentiation-dependent factor 1/sterol regulatory element-binding protein 1c regulates mouse adiponectin expression. *J Biol Chem* **279** (21): 22108-22117 (2004).
31. Lee, J. H. *et al.* SCAP deficiency facilitates obesity and insulin resistance through shifting adipose tissue macrophage polarization. *J Adv Res* **45**: 1-13 (2023).
32. Engin, A. B. Message transmission between adipocyte and macrophage in obesity. *Adv Exp Med Biol* **1460**: 273-295 (2024).
33. Lai, L. *et al.* Longitudinal association between DNA methylation and type 2 diabetes: findings from the KORA F4/FF4 study. *Cardiovasc Diabetol* **24** (1): 19 (2025).
34. Burgess, S. *and* Thompson, S. G. Bias in causal estimates from Mendelian randomization studies with weak instruments. *Stat Med* **30** (11): 1312-1323 (2011).
35. Schoenmaker, M. *et al*. Evidence of genetic enrichment for exceptional survival using a family approach: The Leiden Longevity Study. *Eur J Hum Genet* **14** (1): 79-84 (2006).
36. Sinke, L. *et al.* DNAmArray: Streamlined workflow for the quality control, normalization, and analysis of Illumina methylation array data (2.1) *Zenodo* (2019).
37. Meisinger, C. *et al.* Prevalence of undiagnosed diabetes and impaired glucose regulation in 35-59-year-old individuals in Southern Germany: The KORA F4 study. *Diabet Med* **27** (3): 360-362 (2010).
38. Herder, C. *et al.* Association of subclinical inflammation with polyneuropathy in the older population: KORA F4 study. *Diabetes Care* **36** (11): 3663-3670 (2013).
39. Kriebel, J. *et al.* Association between DNA Methylation in whole blood and measures of glucose metabolism: Kora F4 study. *PLoS One* 11 (3): e0152314 (2016).
40. Touleimat, N. *and* Tost, J. Complete pipeline for Infinium® Human Methylation 450K BeadChip data processing using subset quantile normalization for accurate DNA methylation estimation. *Epigenomics* **4** (3): 325-341 (2012).
41. Costeira, R. *et al.* Metabolomic biomarkers of habitual B vitamin intakes unveil novel differentially methylated positions in the human epigenome. *Clin Epigenetics* **15** (1): 166 (2023).
42. Gentleman, R. C. *et al.* Bioconductor: open software development for computational biology and bioinformatics. *Genome Biol* **5** (10): R80 (2004).
43. Xu, Z. *et al.* ENmix: A novel background correction method for Illumina HumanMethylation450 BeadChip. *Nucleic Acids Res* **44** (3): e20 (2016).
44. Aryee, M. J. *et al.* Minfi: A flexible and comprehensive Bioconductor package for the analysis of Infinium DNA methylation microarrays. *Bioinformatics* **30** (10): 1363-1369 (2014).
45. Christiansen, C. *et al.* Adipose methylome integrativeomic analyses reveal genetic and dietary metabolic health drivers and insulin resistance classifiers. *Genome Med* **14** (1): 75 (2022).
46. Völzke, H. *et al.* Cohort Profile Update: The Study of Health in Pomerania (SHIP). *Int J Epidemiol* **51** (6): e372-e383 (2022).
47. Lehne, B. *et al.* A coherent approach for analysis of the Illumina HumanMethylation450 BeadChip improves data quality and performance in epigenome-wide association studies. *Genome Biol* **16** (1): 37 (2015).
48. Scholtens, S. *et al.* Cohort Profile: LifeLines, a threegeneration cohort study and biobank. *Int J Epidemiol* **44** (4): 1172-1180 (2015).
49. Tigchelaar, E. F. *et al.* Cohort profile: LifeLines DEEP, a prospective, general population cohort study in the northern Netherlands: study design and baseline characteristics. *BMJ Open* **5** (8): e006772 (2015).
50. Lu, X. *et al.* An epigenome-wide association study identifies multiple DNA methylation markers of exposure to endocrine disruptors. *Environ Int* **144**: 106016 (2020).
51. Koestler, D. C. *et al.* Improving cell mixture deconvolution by identifying optimal DNA methylation libraries (IDOL). *BMC Bioinformatics* **17** (1): 120 (2016).
52. Zheng, S. C. *et al.* Identification of differentially methylated cell types in epigenome-wide association studies. *Nat Methods* **15** (12): 1059-1066 (2018).
53. Amemiya, H. M., Kundaje, A. *and* Boyle, A. P. The ENCODE Blacklist: Identification of Problematic Regions of the Genome. *Sci Rep* **9** (1): 9354 (2019).
54. Zhou, W., Laird, P. W. *and* Shen, H. Comprehensive characterization, annotation and innovative use of Infinium DNA methylation BeadChip probes. *Nucleic Acids Res* **45** (4): e22 (2017).
55. van Iterson, M. *et al.* Controlling bias and inflation in epigenome- and transcriptome-wide association studies using the empirical null distribution. *Genome Biol* **18** (1): 19 (2017).
56. Willer, C. J., Li, Y. *and* Abecasis, G. R. METAL: Fast and efficient meta-analysis of genomewide association scans. *Bioinformatics* **26** (17): 2190-2191 (2010).

57. Slieker, R. C. *et al.* Identification and systematic annotation of tissue-specific differentially methylated regions using the Illumina 450k array. *Epigenetics Chromatin* **6** (1): 26 (2013).
58. Battram, T. *et al.* The EWAS Catalog: a database of epigenome-wide association studies. *Wellcome Open Res* **7**: 41 (2022).
59. Li, M. *et al.* EWAS Atlas: A curated knowledgebase of epigenome-wide association studies. *Nucleic Acids Res* **47** (D1): D983-D988 (2019).
60. Heinz, S. *et al.* Simple combinations of lineage-determining transcription factors prime cis-regulatory elements required for macrophage and B cell identities. *Mol Cell* **38** (4): 576-589 (2010).
61. van Greevenbroek, M. M. J. *et al.* The cross-sectional association between insulin resistance and circulating complement C3 is partly explained by plasma alanine aminotransferase, independent of central obesity and general inflammation (the CODAM study). *Eur J Clin Invest* **41** (4): 372-379 (2011).
62. Willemsen, G. *et al.* The Netherlands twin register biobank: A resource for genetic epidemiological studies. *Twin Res Hum Genet* **13** (3): 231-245 (2010).
63. Van Dongen, J. *et al.* Genetic and environmental influences interact with age and sex in shaping the human methylome. *Nat Commun* **7**: 11115 (2016).
64. Hofman, A. *et al.* The Rotterdam Study: 2014 objectives and design update. *Eur J Epidemiol* **28** (11): 889-926 (2013).
65. Huisman, M. H. B. *et al.* Population based epidemiology of amyotrophic lateral sclerosis using capture-recapture methodology. *J Neurol Neurosurg Psychiatry* **82** (10): 1165-1170 (2011).
66. Robinson, M. D., McCarthy, D. J., *and* Smyth, G. K. edgeR: a bioconductor package for differential expression analysis of digital gene expression data. *Bioinformatics* **26** (1): 139-140 (2010).
67. Lawrence, M. *et al.* Software for Computing and Annotating Genomic Ranges. *PLoS Comput Biol* **9** (8): e1003118 (2013).
68. Tini, G. *et al.* DNA methylation during human adipogenesis and the impact of fructose. *Genes Nutr* **15** (1): 21 (2020).
69. Wu, T. *et al.* clusterProfiler 4.0: A universal enrichment tool for interpreting omics data. *Innovation (Camb)* **2** (3): 100141 (2021).
70. Pierce, B. L. and Burgess, S. Efficient design for Mendelian randomization studies: subsample and 2-sample instrumental variable estimators. *Am J Epidemiol* **178** (7): 1177-1184 (2013).
71. Min, J. L. *et al.* Genomic and phenotypic insights from an atlas of genetic effects on DNA methylation. *Nat Genet* **53** (9): 1311-1321 (2021).
72. Sarsani, V. *et al.* A cross-ancestry genome-wide meta-analysis, fine-mapping, and gene prioritization approach to characterize the genetic architecture of adiponectin. *HGG Adv* **5** (1): 100252 (2024).
73. Kilpeläinen, T. O. *et al.* Genome-wide meta-analysis uncovers novel loci influencing circulating leptin levels. *Nat Commun* **7** (1): 1-14 (2016).
74. Machiela, M. J. *and* Chanock, S. J. LDlink: A web-based application for exploring population-specific haplotype structure and linking correlated alleles of possible functional variants. *Bioinformatics* **31** (21): 3555-3557 (2015).

Supplementary Material

CpG	Position	*n*	beta	SE	*p*	p_{FDR}
cg06500161	chr21:43656587	2773	-0.0127	0.0012	5.60E-28	2.31E-22
cg11024682	chr17:17730094	2773	-0.0106	0.0011	3.01E-22	6.20E-17
cg27243685	chr21:43642366	2770	-0.0061	0.0009	1.20E-12	1.65E-07
cg06192883	chr15:52554171	2774	-0.0094	0.0014	4.77E-12	4.92E-07
cg00574958	chr11:68607622	2770	0.0043	0.0007	1.00E-10	8.28E-06
cg07504977	chr10:102131012	2772	-0.0113	0.0018	3.01E-10	2.07E-05
cg01881899	chr21:43652704	2751	-0.0045	0.0007	4.21E-10	2.48E-05
cg00134210	chr10:14644132	2768	0.0040	0.0006	7.90E-10	4.07E-05
cg10717869	chr1:205780912	2768	-0.0057	0.0009	2.44E-09	1.12E-04
cg25217710	chr1:156609523	2775	-0.0052	0.0009	4.64E-09	1.91E-04
cg05945608	chr6:42739639	2773	-0.0072	0.0012	5.76E-09	2.16E-04
cg17901584	chr1:55353706	2775	0.0107	0.0018	7.42E-09	2.55E-04
cg04658841	chr16:85478651	2772	-0.0054	0.0010	1.55E-08	4.92E-04
cg10438589	chr4:14531493	2771	-0.0087	0.0016	2.37E-08	6.97E-04
cg05014727	chr10:6214016	2770	0.0103	0.0019	4.57E-08	1.22E-03
cg02235049	chr3:186559186	2772	-0.0051	0.0009	4.73E-08	1.22E-03
cg13123009	chr6:31681882	2764	-0.0057	0.0011	6.83E-08	1.66E-03
cg20544516	chr17:17717183	2770	-0.0047	0.0009	1.21E-07	2.76E-03
cg06603309	chr11:2724144	2328	0.0059	0.0011	1.72E-07	3.38E-03
cg14476101	chr1:120255992	2759	0.0124	0.0024	1.70E-07	3.38E-03

Supplementary Table 1 | Top 20 CpGs associated with circulating adiponectin levels in blood. CpG identifier, genomic position, sample size (*n*), and association with IL-6 (beta) is shown, alongside standard error (SE) and significance (nominal and FDR-adjusted *p*-value).

CpG	Position	*n*	beta	SE	*p*	p_{FDR}
cg06500161	chr21:43656587	3644	0.0071	0.0006	4.98E-32	2.02E-26
cg00574958	chr11:68607622	3638	-0.0040	0.0004	6.62E-27	1.34E-21
cg14476101	chr1:120255992	3612	-0.0117	0.0012	8.89E-23	1.20E-17
cg17501210	chr6:166970252	3644	-0.0078	0.0008	5.07E-22	5.15E-17
cg11024682	chr17:17730094	3644	0.0051	0.0006	1.41E-19	1.14E-14
cg16246545	chr1:120255941	3638	-0.0085	0.0010	1.41E-18	9.53E-14
cg03725309	chr1:109757585	3638	-0.0049	0.0006	1.29E-16	7.51E-12
cg06192883	chr15:52554171	3646	0.0057	0.0007	5.00E-15	2.54E-10
cg17058475	chr11:68607737	3646	-0.0042	0.0005	1.13E-14	5.09E-10
cg26403843	chr5:158634085	3607	0.0103	0.0014	4.66E-14	1.83E-09
cg06690548	chr4:139162808	3537	-0.0046	0.0006	4.95E-14	1.83E-09
cg17901584	chr1:55353706	3647	-0.0072	0.0010	1.17E-13	3.95E-09
cg27243685	chr21:43642366	3636	0.0031	0.0004	1.94E-13	6.05E-09
cg06559575	chr12:53490352	3643	-0.0043	0.0006	3.34E-13	9.70E-09
cg19750657	chr13:38935967	3643	0.0051	0.0007	1.34E-12	3.62E-08
cg07573872	chr19:1126342	3631	-0.0051	0.0007	1.93E-12	4.91E-08
cg11376147	chr11:57261198	3644	-0.0026	0.0004	2.60E-12	6.21E-08
cg18120259	chr6:43894639	3642	-0.0047	0.0007	3.90E-12	8.81E-08
cg18181703	chr17:76354621	3643	-0.0060	0.0009	4.50E-12	9.62E-08
cg07504977	chr10:102131012	3643	0.0064	0.0009	9.43E-12	1.92E-07

Supplementary Table 2 | Top 20 CpGs associated with circulating leptin levels in blood. CpG identifier, genomic position, sample size (*n*), and association with IL-6 (beta) is shown, alongside standard error (SE) and significance (nominal and FDR-adjusted *p*-value).

Trait	OR	lnOR	SE	p	p_{FDR}	Overlap	%
Body mass index	571.7	6.35	5.15	2.75E-157	2.75E-157	40	54.79
Fasting insulin	435.5	6.08	4.96	5.04E-127	5.04E-127	24	32.88
Triglyceride levels	1917.4	7.56	6.79	4.41E-117	4.41E-117	14	19.18
Waist circumference	372.4	5.92	5.01	3.39E-89	3.39E-89	15	20.55
HDL-cholesterol	465.8	6.14	5.35	8.25E-80	8.25E-80	12	16.44
C-reactive protein	301.3	5.71	5.01	9.11E-61	9.11E-61	10	13.70
Type 2 diabetes	533.8	6.28	5.74	8.76E-59	8.76E-59	8	10.96
Diastolic BP	295.3	5.69	5.21	1.31E-44	1.31E-44	7	9.59
Fasting glucose	121.4	4.80	4.08	1.86E-44	1.86E-44	10	13.70
Systolic BP	215.2	5.37	4.89	2.09E-40	2.09E-40	7	9.59
Age	18.2	2.90	1.73	1.77E-33	1.77E-33	28	38.36
Alcohol	15.9	2.76	1.70	6.57E-26	6.57E-26	20	27.40
Smoking status	11.8	2.46	1.32	1.73E-23	1.73E-23	25	34.25
Sex	8.9	2.19	1.05	1.74E-18	1.74E-18	24	32.88
Dodecanedioate	60.9	4.11	4.00	1.84E-15	1.84E-15	4	5.48
Parkinson's disease	102.1	4.63	4.74	7.20E-15	7.20E-15	3	4.11
Cognition	52.2	3.96	3.84	1.86E-14	1.86E-14	4	5.48
Total cholesterol	181.4	5.20	5.68	8.97E-13	8.97E-13	2	2.74
Dihomo-linolenate	98.4	4.59	5.05	2.19E-10	2.19E-10	2	2.74
PCB exposure	35.5	3.57	3.68	1.57E-09	1.57E-09	3	4.11

Supplementary Table 3 | Top 20 traits from EWAS enrichment analysis. Odds ratio of enrichment in adiponectin-associated CpGs (OR and log-transformed lnOR) is shown, alongside its standard error (SE) and significance (nominal and FDR-adjusted *p*-value). The overlap (total and percentage) with adiponectin-associated CpGs is also presented.

Trait	OR	lnOR	SE	p	p_{FDR}	Overlap	%
Body mass index	151.3	5.02	3.38	1.09E-204	1.09E-204	51	24.17
Fasting insulin	147.5	4.99	3.60	4.05E-134	4.05E-134	30	14.22
C-reactive protein	256.7	5.55	4.30	6.97E-131	6.97E-131	24	11.37
Triglyceride levels	413.7	6.03	5.29	5.75E-71	5.75E-71	11	5.21
Systolic BP	137.4	4.92	4.01	1.90E-62	1.90E-62	13	6.16
Smoking	9.8	2.28	0.53	3.18E-52	3.18E-52	64	30.33
Alcohol	11.7	2.46	0.84	5.60E-49	5.60E-49	46	21.80
Diastolic BP	127.4	4.85	4.16	2.05E-43	2.05E-43	9	4.27
HDL-cholesterol	102.8	4.63	3.94	3.14E-40	3.14E-40	9	4.27
Waist circumference	69.9	4.25	3.48	4.72E-38	4.72E-38	10	4.74
Sex	6.0	1.80	0.12	9.63E-30	9.63E-30	53	25.12
Cognition	40.4	3.70	2.99	5.48E-27	5.48E-27	9	4.27
Type 2 diabetes	100.6	4.61	4.33	2.71E-23	2.71E-23	5	2.37
Mortality	11.4	2.44	1.44	1.54E-18	1.54E-18	14	6.64
Age	5.2	1.65	0.20	8.38E-18	8.38E-18	32	15.17
Fasting glucose	22.0	3.09	2.65	1.16E-13	1.16E-13	6	2.84
Education level	27.3	3.31	3.00	3.98E-13	3.98E-13	5	2.37
Protein biomarker	42.4	3.75	3.85	1.80E-10	1.80E-10	3	1.42
Parkinson's disease	33.9	3.52	3.62	1.91E-09	1.91E-09	3	1.42
Total cholesterol	60.7	4.11	4.57	1.25E-08	1.25E-08	2	0.95

Supplementary Table 4 | Top 20 traits from EWAS enrichment analysis. Odds ratio of enrichment in leptin-associated CpGs (OR and log-transformed lnOR) is shown, alongside its standard error (SE) and significance (nominal and FDR-adjusted *p*-value). The overlap (total and percentage) with leptin-associated CpGs is also presented.

Chromatin State	OR	lnOR	SE	p	p_{FDR}	Full Roadmap name
(1) TssA	0.17	-1.79	-0.64	7.47E-02	2.24E-01	Active TSS
(2) TssAFlnk	0.56	-0.59	-1.18	1.18E-01	2.53E-01	Flanking active TSS
(3) TxFlnk	5.08	1.63	2.78	1.07E-01	2.53E-01	Transcr. at gene 5' and 3'
(4) Tx	2.08	0.73	-0.14	1.67E-02	1.25E-01	Strong transcription
(5) TxWk	1.05	0.05	-0.46	9.09E-01	9.57E-01	Weak transcription
(6) EnhG	0.00	-8.92	113.23	8.87E-01	9.57E-01	Genic enhancers
(7) Enh	8.82	2.18	1.15	1.12E-15	1.69E-14	Enhancers
(8) ZNF/Rpts	0.00	-9.21	323.98	9.57E-01	9.57E-01	ZNF genes + repeats
(9) Het	0.00	-8.63	113.52	8.91E-01	9.57E-01	Heterochromatin
(10) TssBiv	1.99	0.69	0.57	1.82E-01	3.42E-01	Bivalent/poised TSS
(11) BivFlnk	0.00	-9.09	64.73	8.11E-01	9.57E-01	Flanking bivalent TSS/Enh
(12) EnhBiv	0.00	-9.43	112.72	8.80E-01	9.57E-01	Bivalent enhancer
(13) ReprPC	0.27	-1.31	-0.87	6.66E-02	2.24E-01	Repressed polycomb
(14) ReprPCWk	0.22	-1.50	-1.06	3.55E-02	1.78E-01	Weak repressed polycomb
(15) Quies	1.09	0.08	-0.92	7.61E-01	9.57E-01	Quiescent/low

Supplementary Table 5 | Chromatin state enrichment analysis results using the peripheral blood mononuclear cell reference epigenome (PBMC; E062). The odds ratio of enrichment in adiponectin-associated CpGs (OR and log-transformed lnOR) is shown, alongside its standard error (SE) and significance (nominal and FDR-adjusted *p*-value). The abbreviated and full Roadmap names are also displayed (TSS: transcription start site, ZNF: zinc finger).

Chromatin State	OR	lnOR	SE	p	p_{FDR}	Full Roadmap name
(1) TssA	0.64	-0.44	-1.29	1.55E-01	2.91E-01	Active TSS
(2) TssAFlnk	0.73	-0.32	-1.74	1.09E-01	2.72E-01	Flanking active TSS
(3) TxFlnk	5.21	1.65	1.73	4.60E-03	2.03E-02	Transcr. at gene 5' and 3'
(4) Tx	0.67	-0.40	-1.41	1.45E-01	2.91E-01	Strong transcription
(5) TxWk	1.92	0.65	-0.85	4.03E-04	3.02E-03	Weak transcription
(6) EnhG	1.98	0.68	0.53	1.77E-01	2.95E-01	Genic enhancers
(7) Enh	4.87	1.58	0.11	6.23E-17	9.35E-16	Enhancers
(8) ZNF/Rpts	0.00	-10.17	309.90	9.50E-01	9.50E-01	ZNF genes + repeats
(9) Het	1.39	0.33	0.76	6.45E-01	8.73E-01	Heterochromatin
(10) TssBiv	0.00	-10.04	60.86	7.83E-01	8.86E-01	Bivalent/poised TSS
(11) BivFlnk	0.30	-1.20	-0.77	9.03E-02	2.71E-01	Flanking bivalent TSS/Enh
(12) EnhBiv	0.88	-0.13	-0.05	8.27E-01	8.86E-01	Bivalent enhancer
(13) ReprPC	0.37	-1.00	-1.65	5.41E-03	2.03E-02	Repressed polycomb
(14) ReprPCWk	0.86	-0.15	-1.39	5.04E-01	7.55E-01	Weak repressed polycomb
(15) Quies	1.06	0.06	-1.59	6.99E-01	8.73E-01	Quiescent/low

Supplementary Table 6 | Chromatin state enrichment analysis results using the peripheral blood mononuclear cell reference epigenome (PBMC; E062). The odds ratio of enrichment in leptin-associated CpGs (OR and log-transformed lnOR) is shown, alongside its standard error (SE) and significance (nominal and FDR-adjusted *p*-value). The abbreviated and full Roadmap names are also displayed.

Trait	TF	*p*	p_{FDR}	CpG *n*	CpG %	Background %
Leptin	RFX (HTH)	1.12E-08	1.57E-07	4	1.86	0.15
Leptin	Fosl2 (bZIP)	3.11E-08	2.18E-07	6	2.79	0.46
Leptin	Rfx2 (HTH)	9.98E-08	4.66E-07	4	1.86	0.20
Adiponectin	MafA (bZIP)	1.91E-07	6.69E-07	7	9.59	2.22
Leptin	JunB (bZIP)	2.61E-07	7.31E-07	7	3.26	0.76
Leptin	Rfx1 (HTH)	5.41E-07	1.26E-06	5	2.33	0.40
Leptin	AP-1 (bZIP)	1.42E-06	2.66E-06	8	3.72	1.10
Leptin	Bach2 (bZIP)	1.52E-06	2.66E-06	4	1.86	0.27
Leptin	BATF (bZIP)	2.51E-06	3.90E-06	7	3.26	0.90
Leptin	SCL (bHLH)	4.33E-06	6.06E-06	48	22.33	15.41
Leptin	X-box (HTH)	6.95E-06	8.85E-06	3	1.40	0.17
Adiponectin	Npas4 (bHLH)	1.04E-05	1.21E-05	7	9.59	3.05
Adiponectin	Zic3 (Zf)	1.39E-05	1.50E-05	5	6.85	1.68
Leptin	KLF6 (Zf)	2.06E-05	2.06E-05	14	6.51	3.17

Supplementary Table 7 | Transcription factor (TF) binding site enrichment analysis results. Sequences within 50bp of adipokine-associated CpGs were scanned for established motifs using HOMER and compared to a random genomic background matched for GC content. TF name and type are shown alongside the significance of the enrichment (nominal and FDR-adjusted *p*-values). The number of CpGs responsible for the enrichment are also displayed (CpG *n*, CpG %), as well as the percentage of background sequences within 50bp of the respective motif.

CpG	Gene name	Ensembl ID	beta	*p*	p_{FDR}	Nearest
cg14476101	*PHGDH*	ENSG00000092621	-0.0401	3.37E-129	9.90E-127	TRUE
cg17901584	*DHCR24*	ENSG00000116133	-0.0208	1.39E-80	2.05E-78	FALSE
cg06500161	*ABCG1*	ENSG00000160179	-0.0114	1.75E-61	1.72E-59	FALSE
cg17194270	*SYNGR1*	ENSG00000100321	-0.0128	6.85E-42	5.04E-40	FALSE
cg27243685	*ABCG1*	ENSG00000160179	-0.0069	3.02E-31	1.78E-29	FALSE
cg01881899	*ABCG1*	ENSG00000160179	-0.0048	3.59E-25	1.76E-23	FALSE
cg20496314	*SYNGR1*	ENSG00000100321	-0.0082	8.95E-25	3.76E-23	FALSE
cg00574958	*CPT1A*	ENSG00000110090	-0.0039	1.12E-24	4.12E-23	FALSE
cg03234777	*MPZL2*	ENSG00000149573	0.0059	2.64E-24	8.61E-23	FALSE
cg11024682	*SREBF1*	ENSG00000072310	-0.0060	1.31E-18	3.84E-17	FALSE
cg03234777	*MPZL3*	ENSG00000160588	0.0048	3.09E-16	8.27E-15	TRUE
cg14117297	*TMIGD2*	ENSG00000167664	-0.0043	4.05E-14	9.93E-13	FALSE
cg10192877	*ABCG1*	ENSG00000160179	-0.0032	4.73E-14	1.07E-12	FALSE
cg00134210	*FAM107B*	ENSG00000065809	-0.0031	1.69E-12	3.54E-11	FALSE
cg11024682	*TOM1L2*	ENSG00000175662	-0.0041	3.87E-10	7.58E-09	FALSE
cg23594345	*IGHD6-25*	ENSG00000225825	0.0099	2.18E-09	4.01E-08	FALSE
cg26949393	*AGAP3*	ENSG00000133612	0.0018	6.39E-07	1.11E-05	FALSE
cg20544516	*SREBF1*	ENSG00000072310	-0.0034	8.25E-07	1.35E-05	TRUE
cg03234777	*AMICA1*	ENSG00000160593	-0.0030	1.33E-06	2.00E-05	FALSE
cg11147309	*PLEC*	ENSG00000178209	-0.0029	1.36E-06	2.00E-05	TRUE

Supplementary Table 8 | Top 20 expression quantitative trait methylation (eQTM) effects connecting adiponectin-associated CpGs and nearby genes (within 100kb), ordered by *p*-value. The CpG and gene identifiers are shown alongside their eQTM effect size and significance.

CpG	Gene name	Ensembl	beta	*p*	p_{FDR}	Nearest
cg07639376	*TMEM204*	ENSG00000131634	-0.0860	1.45E-247	1.18E-244	TRUE
cg14476101	*PHGDH*	ENSG00000092621	-0.0401	3.37E-129	1.37E-126	TRUE
cg05668853	*RAB34*	ENSG00000109113	-0.0201	2.87E-112	7.79E-110	TRUE
cg16246545	*PHGDH*	ENSG00000092621	-0.0289	1.27E-109	2.58E-107	TRUE
cg17901584	*DHCR24*	ENSG00000116133	-0.0208	1.39E-80	2.27E-78	FALSE
cg06500161	*ABCG1*	ENSG00000160179	-0.0114	1.75E-61	2.38E-59	FALSE
cg10045881	*CHI3L2*	ENSG00000064886	-0.0105	5.35E-43	6.23E-41	TRUE
cg23361127	*ENC1*	ENSG00000171617	-0.0079	1.56E-38	1.59E-36	FALSE
cg17332198	*METTL21B*	ENSG00000123427	-0.0060	5.30E-34	4.80E-32	FALSE
cg18149207	*RORC*	ENSG00000143365	-0.0060	4.95E-29	4.03E-27	FALSE
cg22650271	*SYNGR1*	ENSG00000100321	-0.0066	1.96E-27	1.45E-25	FALSE
cg20496314	*SYNGR1*	ENSG00000100321	-0.0082	8.95E-25	6.08E-23	FALSE
cg00574958	*CPT1A*	ENSG00000110090	-0.0039	1.12E-24	7.03E-23	FALSE
cg18930267	*NOC4L*	ENSG00000184967	-0.0078	7.65E-24	4.45E-22	TRUE
cg13871708	*VARS2*	ENSG00000137411	0.0079	5.00E-20	2.71E-18	FALSE
cg17058475	*CPT1A*	ENSG00000110090	-0.0046	8.18E-19	4.17E-17	FALSE
cg02741985	*CCDC57*	ENSG00000176155	-0.0057	1.50E-18	7.20E-17	TRUE
cg11468085	*ACY3*	ENSG00000132744	-0.0056	1.22E-16	5.51E-15	FALSE
cg23361127	*HEXB*	ENSG00000049860	-0.0056	1.94E-15	8.34E-14	FALSE
cg22534374	*NAV1*	ENSG00000134369	-0.0074	1.16E-13	4.72E-12	FALSE

Supplementary Table 9 | Top 20 expression quantitative trait methylation (eQTM) effects connecting leptin-associated CpGs and nearby genes (within 100kb), ordered by *p*-value. The CpG and gene identifiers are shown alongside their eQTM effect size and significance.

Database	Gene set	Size	Overlap	*p*	p_{FDR}
GeDiPNet (2023)	Micromelia	102	7	6.89E-07	2.42E-03
PheWeb (2019)	Hereditary and idiopathic peripheral neuropathy	18	4	1.55E-06	2.71E-03
WikiPathway (2021)	Cholesterol metabolism (includes both Bloch and Kandutsch-Russell pathways)	46	5	2.94E-06	3.30E-03
Elsevier Pathway Collection	Proteins with Altered Expression in Cancer Metabolic Reprogramming	85	6	3.76E-06	3.30E-03
Elsevier Pathway Collection	Glutamine in Cancer Metabolism	28	4	9.96E-06	6.99E-03
Reactome (2022)	Metabolism Of Lipids R-HSA-556833	732	14	1.40E-05	8.21E-03
Reactome (2022)	Metabolism R-HSA-1430728	2049	25	1.73E-05	8.67E-03
BioPlanet (2019)	Oncostatin M	311	9	2.25E-05	9.86E-03
WikiPathway (2021)	Nuclear Receptors Meta-Pathway	319	9	2.74E-05	1.07E-02
BioPlanet (2019)	Transmembrane transport of small molecules	432	10	5.24E-05	1.75E-02
MsigDB (2020)	Xenobiotic Metabolism	200	7	5.75E-05	1.75E-02
BioPlanet (2019)	Amino acid biosynthesis and interconversion (transamination)	16	3	5.99E-05	1.75E-02
GO BP (2023)	Phosphatidylcholine Metabolic Process (GO:0046470)	55	4	1.50E-04	4.05E-02
Reactome (2022)	Immune System R-HSA-168256	1943	22	1.74E-04	4.37E-02
KEGG (2021)	Insulin resistance	108	5	1.88E-04	4.39E-02

Supplementary Table 10 | Enriched terms in genes linked to leptin-associated CpGs, ordered by *p*-value. The set size and overlap is shown alongside their significance (nominal and FDR-adjusted *p*-value).

Database	Gene set	Size	Overlap	p	p_{FDR}
PheWeb (2019)	Type 1 diabetes	95	7	4.31E-11	5.17E-08
PheWeb_(2019)	Type 1 diabetes with renal manifestations	64	5	2.33E-08	1.40E-05
Elsevier Pathway Collection	Proteins with Altered Expression in Cancer Metabolic Reprogramming	85	5	9.81E-08	3.92E-05
PheWeb (2019)	Celiac disease	90	5	1.31E-07	3.92E-05
WikiPathway (2021)	Cholesterol metabolism (includes both Bloch and Kandutsch-Russell pathways) WP4718	46	4	4.23E-07	1.02E-04
Elsevier Pathway Collection	Metabolic Effects of Oncogenes and Tumor Suppressor in Cancer Cells	68	4	2.07E-06	4.14E-04
KEGG (2021)	AMPK signalling pathway	120	4	1.98E-05	3.40E-03
Reactome (2022)	Signalling By Nuclear Receptors R-HSA-9006931	260	5	2.40E-05	3.61E-03
Reactome (2022)	NR1H2 And NR1H3-mediated Signalling R-HSA-9024446	46	3	3.20E-05	4.27E-03
Elsevier Pathway Collection	Estrogen Deficiency in Female Obesity	9	2	6.20E-05	6.77E-03
Reactome (2022)	NR1H2 And NR1H3 Regulate Gene Expression Linked To Lipogenesis R-HSA-9029558	9	2	6.20E-05	6.77E-03
WikiPathway (2021)	Liver X receptor pathway WP2874	10	2	7.75E-05	7.75E-03
BioPlanet (2019)	AMPK signalling	68	3	1.03E-04	9.07E-03
WikiPathway (2021)	AMP-activated protein kinase (AMPK) signalling WP1403	69	3	1.08E-04	9.07E-03
Elsevier Pathway Collection	Lipodystrophy, Familial Partial	12	2	1.13E-04	9.07E-03
GO BP (2023)	Membrane Depolarization During Action Potential (GO:0086010)	13	2	2.53E-06	1.16E-03
PheWeb (2019)	Open-angle glaucoma	13	2	2.80E-06	1.21E-03
MsigDB (2020)	mTORC1 Signalling	200	4	3.33E-06	1.34E-03
GO BP (2023)	High-Density Lipoprotein Particle Remodelling (GO:0034375)	15	2	3.49E-06	1.34E-03
GO BP (2023)	Regulation Of Cholesterol Biosynthetic Process (GO:0045540)	15	2	3.92E-06	1.44E-03

Supplementary Table 11 | Top 20 enriched terms in genes linked to adiponectin-associated CpGs, ordered by *p*-value. The set size and overlap is shown alongside their significance (nominal and FDR-adjusted *p*-value).